Fundamentals of Green Hydrogen through Photocatalysis

Current Insights into Scalability

Ravi Anusuyadevi, P.; Pranavi, Sindhu; Darsi, Jaya Prasanna Kumar; Misra, Yash; Mentha, Spandana Samyuktalakshmi; Gonugunta, P.; Taheri, P.; Mol, J.M.C.

DOI
10.1021/bk-2024-1467.ch007

Publication date
2024

Document Version
Final published version

Published in
Towards Sustainable and Green Hydrogen Production by Photocatalysis

Chapter 7

Fundamentals of Green Hydrogen through Photocatalysis - Current Insights into Scalability

Prasaanth Ravi Anusuyadevi,[1,*] Sindhu Pranavi,[2] Darsi Jaya Prasanna Kumar,[2] Yash Misra,[2] Spandana Samyuktalakshmi Mentha,[2] Prasad Gonugunta,[1] Peyman Taheri,[1] and Arjan Mol[1]

[1]Materials Science and Engineering Department (MSE), Faculty of Mechanical, Maritime and Materials Engineering (3mE), Delft University of Technology, 2628 CD Delft, The Netherlands

[2]Department of Chemical Engineering, M.S. Ramaiah Institute of Technology, Bengaluru 560054, India

[*]E-mail: P.RaviAnusuyadevi@tudelft.nl; ranu.prasaanth@gmail.com

Hydrogen gained momentum as a viable alternative to crude-derived fuels. Scalable production of green hydrogen harnessing solar energy emerged as one of the promising sustainable options that can be facilitated by photocatalyst-assisted water splitting. One-step and two-step photoexcitation systems for overall water splitting (OWS) processes gained much importance because of the ease with which they can be scaled up. This chapter gives a profound insight into the fundamental aspects of these systems, along with a broader picture regarding their possible pathway for commercial implementation. Thermodynamic and kinetic requisites of these novel systems have been described in detail and a critical appraisal of the selectivity of co-catalysts in the photocatalytic OWS process is presented. Subsequently, this chapter provides a comprehensive focus on various novel scalability studies like thin film systems, baggie reactors and the solar hydrogen farm project. The ultimate motive of this chapter is to summarize the current state-of-the-art strategies for producing green hydrogen through heterogeneous photocatalysis and the various limitations it possesses that preclude the system from reaching the market so far. By this it will motivate people to develop innovative pathways that would rectify the problems associated with it.

Introduction to Green Hydrogen

In the period of augmenting fuel prices, depleting fossil-based reserves, global climatic change, pollution of natural resources and surging energy consumption due to population, the scalable realization of renewable energy sources has become the need of the hour (*1*). In the futuristic direction of renewable energy utilization, production and usage of hydrogen (H_2) gas is seen as

Kumar; Towards Sustainable and Green Hydrogen Production by Photocatalysis: Scalability Opportunities and Challenges (Volume 1)
ACS Symposium Series; American Chemical Society: Washington, DC, 0.

the most desirable option. As this (H_2) stands as a clean fuel, releasing no greenhouse gases after its combustion. Importantly, it possesses very high energy content, of about 0.122 MJ/g and its corresponding energy yield is 2.75 times more than the energy delivered by fossil fuels (hydrocarbons) (*2*). H_2 has a high gravimetric heating value (141.9 MJ/kg) compared to crude-derived fuels: methane (55.5 MJ/kg), petrol (47.5 MJ/kg), diesel (44.8 MJ/kg) and methanol (20 MJ/kg) (*3*). Thus making it as a green alternative for exhausting traditional fuels and a potential renewable energy carrier (*4*).

Still, H_2 is not facilely and immediately available from natural sources. It is derived from hydrogen-containing materials using myriad energy sources. However, the major fraction of H_2 produced is industrially derived from fossil fuels, which suffer a huge release of carbon dioxide (CO_2) into the atmosphere. This has led to an incentive for establishing sustainable H_2 producing pathways from renewable resources. Among the renewable and non-renewable energy sources, solar energy is the most dominant one with 173000 terawatts (TW) of energy reaching the surface of the earth continuously from the sun. This is roughly 9600 times higher than the current energy consumption of the world (*3*).

Sustainably, H_2 is generated from solar energy through three different techniques: (i) Photoelectrochemical cells, (ii) Photovoltaic (PV) coupled-electrolysis, and (iii) Heterogeneous Particulate Photocatalysis. The rudimentary mechanism of H_2 generation is the splitting of water molecules into H_2 and oxygen (O_2) gases. Among these techniques, the least expensive and easily scalable process is the particulate photocatalysis system, since the solar photon absorption, catalysis and production of H_2 all occur on the surface of the photocatalysts. The calculated norm price of H_2 from a particulate photocatalytic system will be in the range of 1.6–3.5 $/kg, if we use a photocatalytic system delivering STH (solar-to-hydrogen) conversion efficiency in the range of 5–10% with a durability (lifetime) of 5 years (*5*).

Regardless of the propensity of the particulate photocatalytic system for scale-up and immediate commercialization, the photocatalysts developed so far fall short of the requisite STH efficiency. Thus, this chapter describes the fundamental mechanism of water splitting with powder-based semiconductor photocatalytic systems and profoundly points out the challenges it constitutes, precluding it from large scale implementation. Finally, this chapter reveals the prospective for large scale implementation and the multi-disciplinary research required from both material science and chemical engineering research communities for successfully developing the photocatalytic systems for generating hydrogen.

Fundamental Requisites for Green Hydrogen Production through Photocatalytic Water Splitting Reaction

H_2 produced from a technology that meets sustainable criteria can be termed as 'green' hydrogen. In this perspective, H_2 generated through photocatalytic system can be termed as green H_2, as it employs renewable solar energy and sustainable water molecules (*6*). The facile and economical way to produce hydrogen is through splitting the water molecule using photonic or electrical energy. The large overpotential associated with hydrogen evolution reaction (HER) in the water splitting processes can be lowered with efficient usage of photocatalysts or electrocatalysts, depending on the technique employed. The overall water splitting process is literally composed of

Kumar; Towards Sustainable and Green Hydrogen Production by Photocatalysis: Scalability Opportunities and Challenges (Volume 1)
ACS Symposium Series; American Chemical Society: Washington, DC, 0.

two half-cell reactions, primary and the initial one is water oxidation reaction involving the oxygen (O_2) evolution and the later one involves the reduction of protons [H^+] into hydrogen (H_2).

The overall water splitting reaction(s) is an endergonic (as well as endothermic) process and a non-spontaneous procedure, involving a positive Gibbs free energy change ($\Delta G>0$). Specifically, one mole of water requires a standard Gibbs free energy change (ΔG^o) of 237.2 kJ to disintegrate into H_2 and O_2 molecules (*3*, *7*). The values of thermodynamic state functions involved in the water splitting process are provided in equation (1). From which, it is obvious that only at a temperature higher than 1800 K (>1527 °C), ΔG will be zero, leading to the splitting of water through thermolysis. At ambient conditions, according to ΔG^o, the requisite thermodynamic energy for hydrogen production from water splitting can be provided by an electrochemical cell of a minimum cell voltage of 1.23 eV.

$$H_2O_{(l)} \rightarrow H_2 + O_2\,; \Delta G^o = 237.2\,kJ/mol\,, \Delta H^o = 286\,kJ/mol\,, \Delta S = 163\ J/K\,mol \quad \textbf{(1)}$$

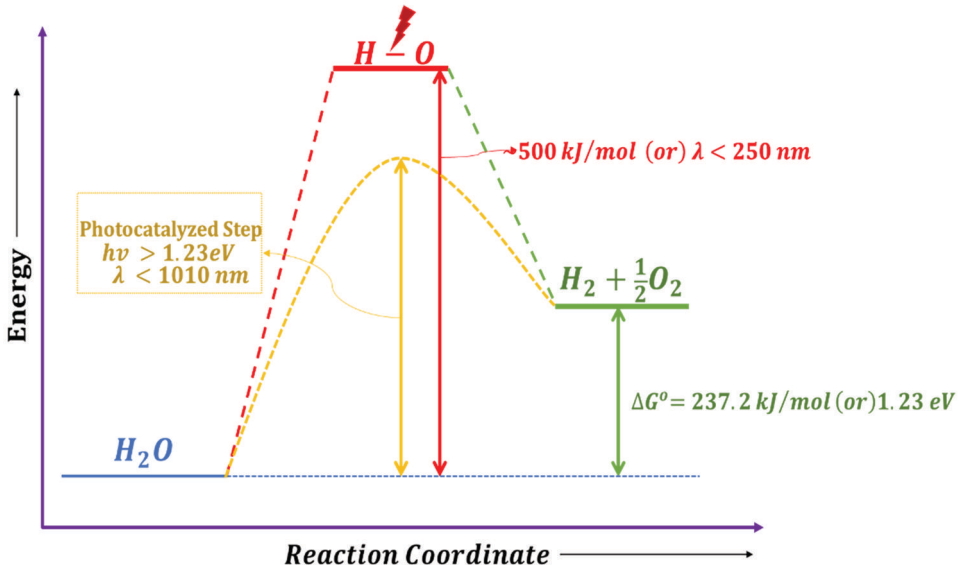

Figure 1. Energy requisites for water splitting reactions through non-catalytic and photocatalytic processes.

In case of dissociation of water molecules, only through exposure to light irradiations, breakage of the first of the two O-H bonds requires an energy input of ~500 kJ/mol, which means exposure to photons with wavelength less than 250 nm is needed (*8*, *9*), schematically depicted in Figure 1. To achieve a process of water splitting, within the regime of sustainability, targeting the utilization of abundant solar energy, photocatalysis using semiconductor particles provides us the path to achieve it facilely. Ideally, the particulate semiconductor photocatalysts with a minimum band gap of E_g>1.23 eV, exhibit the potential to absorb photons with wavelength less than, $\lambda < 1010$ nm (*10*, *11*). Subsequently, semiconductor upon absorption of photons, excites the electron from its valence band (VB) energy level to its conduction band (CB) energy level. These photo-excited charge carriers reach the respective redox sites and perform the overall water splitting. However, for the semiconductor (photocatalysts) to perform the overall water splitting (OWS) process, band gap alone is not the only criterion to be satisfied. The corresponding conduction band (CB) and valence

band (VB) of the photocatalysts should be appropriately positioned at ideal energy levels for the redox reactions of OWS to occur.

The two half redox reactions in the OWS process: (i) Oxygen generation through four-electron oxidation of water molecules, see equation (2) and (ii) Hydrogen generation through two-electron reduction of protons, see equation (3). For the successful realization of OWS through photocatalysis, the valence band of the semiconductor-photocatalysts should be positioned at a potential more positive than the oxidation potential of H_2O to O_2 [E_{O_2/H_2O}=1.23=1.23 eV vs Normal Hydrogen Electrode (NHE)], at pH=0. Simultaneously, the conduction band edge should be positioned at a potential more negative than the reduction potential of proton (H^+) to H_2 ($E_{H^+/H_2} = 0\ eV\ vs\ NHE$), at pH=0 (*12*).

$$2H_2O_{(l)} + 4h^+(or)\ 2H_2O_{(l)} - 4e^- \rightarrow O_{2(g)} + 4H^+ \qquad E_{O_2/H_2O} = 1.23\ eV \quad \textbf{(2)}$$

$$2H^+ + 2e^- \rightarrow H_{2(g)} \qquad E_{H^+/H_2} = 0\ eV \quad \textbf{(3)}$$

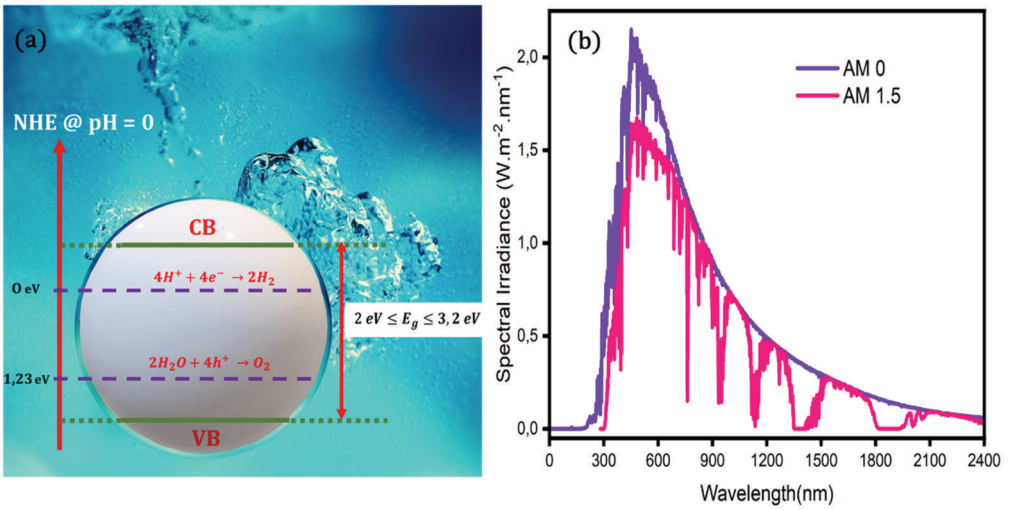

Figure 2. (a) Ideal photocatalysts for overall water splitting; (b) Solar Spectra irradiance: Air Mass (AM) 0-Extra Terrestrial Solar Spectrum; AM 1.5- Hemispherical Titled Solar Spectrum.

Nevertheless, the photocatalytic-OWS process is a heterogenous chemical reaction, occurring on the surface of the solid semiconductor photocatalysts. Thus, the H_2 generation from the photocatalytic surface is associated with an inevitable energy loss due to the electron transfer steps, resulting in a kinetic overpotential. Hence, an overpotential of -0.41 eV on top of 0 eV vs NHE at pH=0, is required to produce H_2 from water molecules (*9*, *12*). Therefore, for the facile production of H_2, the conduction band edge should be positioned more negative than -0.41 eV vs NHE. Similarly, considering the kinetic overpotential associated with the O_2 evolution reaction, the band gap (E_g=Conduction Band Edge Potential [E_{CB}]–Valence Band Edge Potential (E_{VB})] of the semiconductor photocatalysts should be equal or greater than 2 eV (*13*). Concurrently, in order to render the effective usage of the visible portion ($380 < \lambda < 700$ nm) of the solar spectrum (see Figure 2b) for green hydrogen production, E_g of the photocatalysts should be equal or less than 3.2 eV, systematically depicted in Figure 2a. In Figure 2b solar spectra with Air Mass (AM) 0 and 1.5 are

displayed. The data for AM 0 and AM 1.5 was procured from ASTM E490-22 (*14*) and ASTM G173-23 (*15*), standards, respectively.

Finally, in addition to all the above conditions, the photocatalysts employed should also exhibit exalted photo-corrosion stability against the continuous exposure to myriad wavelength of irradiations.

Role of Co-catalysts for Achieving Selectivity in Photocatalytic-OWS Process

The OWS process for the generation of green hydrogen based on particulate photocatalysts can be termed as 'artificial photosynthesis', as it enables us to convert solar energy into energy-rich (hydrogen) molecules. As shown in Figure 1, the products of photocatalytic-OWS process possess higher Gibbs free energy than their reactants and hence their reverse reaction is highly favorable ($\Delta G<0$). Thus, effective photocatalysts employed for OWS-process should not only absorb photons and excite electrons from valence band (VB) into the conduction band (CB) for the green hydrogen production. It should also suppress the direct reverse reaction of H_2 and O_2 to form water. So far, the OWS-process have been successfully realized in the Gallium Nitride (GaN)-based solid solution photocatalysts (*16*), heterostructure of Indium Gallium Nitride (InGaN)/GaN nanorod photocatalysts (*17*) and large number of other metal-oxide based semiconductor particulate-based nanophotocatalysts (*18*, *19*). Since the product mixture (H_2 and O_2) is metastable on the photocatalyst surface and the forward reaction of OWS is very fast compared to the direct-reverse reaction of the products (*20*). The photocatalysts implemented in the above process are synthesized by both bottom-up and top-down approaches in batch mode conditions, delivering low-quantity of photocatalysts (<2 g), not suitable for large-scale exploration. Thanks to the progression in the supercritical-based millifluidics-chemical reactors, this year, continuous synthesis of 2-3 g of GaN nanophotocatalysts per day, was reported (*21*). With such technological advancement, continuous supercritical synthesis ensures large-scale production of nano-photocatalysts, meeting the requirements for scalability of hydrogen production.

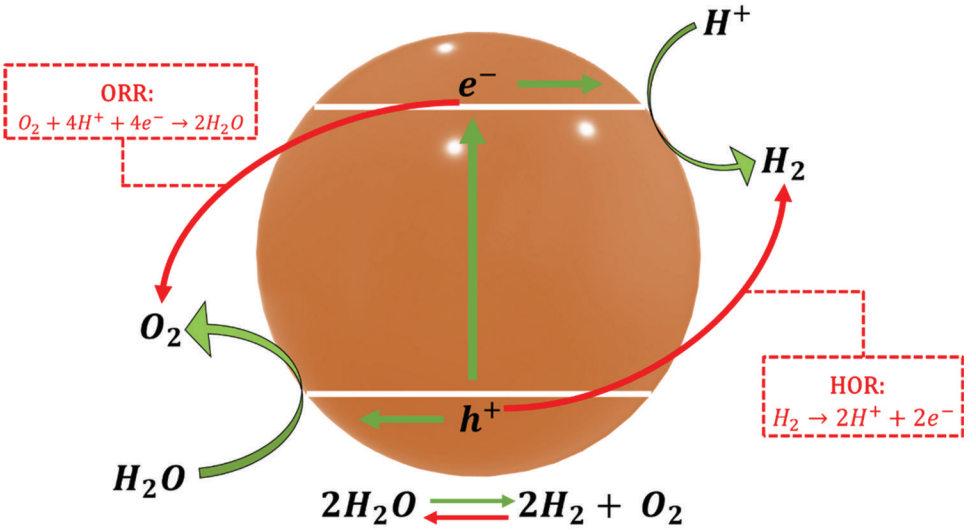

Figure 3. The forward OWS-process on heterogenous photocatalysts surface, indicated by green arrows. The indirect back reactions: 1. Hydrogen Oxidation Reaction (HOR) and 2. Oxygen Reduction Reaction(ORR), ultimately leading to the reversal of OWS-process, indicated by red arrows.

Kumar; Towards Sustainable and Green Hydrogen Production by Photocatalysis: Scalability Opportunities and Challenges (Volume 1)
ACS Symposium Series; American Chemical Society: Washington, DC, 0.

It is highly important to point out to the readers that the photocatalysts' examples specifically mentioned above correspond to '*unmodified*' semiconductors. Here, the term, '*unmodified*' indicates that the semiconductor surface does not contain nor is coated/loaded with supplementary materials that serve as *co-catalysts* for OWS processes. Howbeit, in the OWS process based on heterogeneous photocatalysis, as soon as the H_2 and O_2 evolve on the surface of the photocatalysts, these gaseous products exhibit the propensity to react with the holes of the VB and electrons of CB on the surface, ultimately leading to Hydrogen Oxidation Reaction (HOR) and Oxygen Reduction Reaction(ORR), respectively. These two reactions (HOR and ORR) can indirectly reverse the OWS-process on a photocatalytic surface (Figure 3).

Advancement of the forward reactions pertaining to the OWS-process and complete suppression of the above indirect reverse reactions can be achieved by two distinct paths/designs. The former pertains to the spatial separation of both the half reactions of the OWS process, here, they are carried out in two different compartments and the products of the half reactions do not come in direct contact with each other nor with the incorrect excited charge-carries. This path, where the OWS-process employs two different semiconductor photocatalytic materials for oxidation and reduction half reaction of water, can be termed as *two-step photoexcitation systems* (Z-scheme systems). There are several sub-systems belonging to the path of spatial separation of half-reactions of OWS-processes (for example: Solar Farm project).

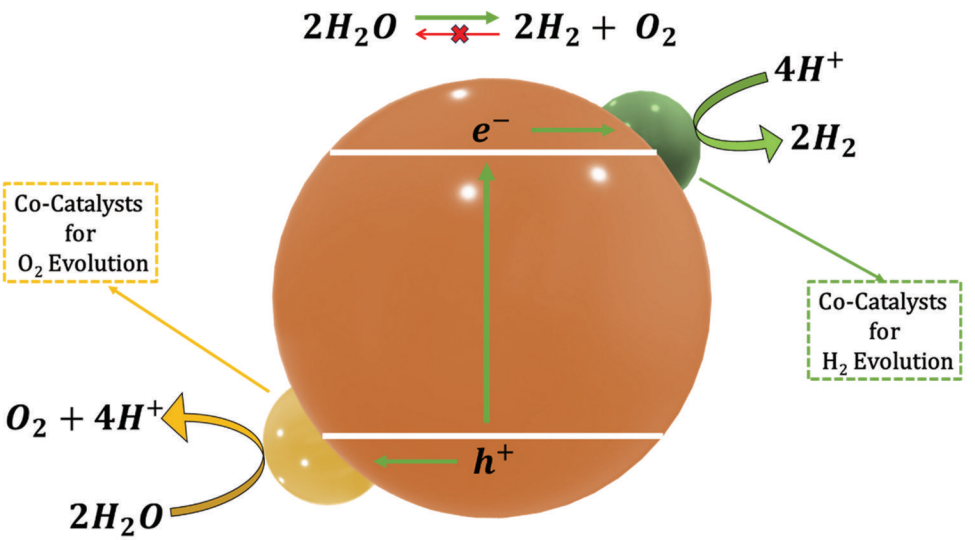

Figure 4. Schematic representation of the photocatalysts loaded with different co-catalysts, employed for one-step photoexcitation-based OWS Process. Charge transfer selectivity attained through co-catalysts suppress the unwanted reverse reactions (HOR and ORR).

In the later strategy, reactants (water), products (H_2 and O_2) and excited charge carriers are not separated from each other. Still, the indirect back reactions are suppressed by successively instigating/establishing charge transfer selectivity (*20*). Such intriguing selectivity is accomplished by loading and/or chemical modification of the photon absorbing semiconductor surface with a different metal and/or metal-oxide material. These different auxiliary materials, termed co-catalysts, provide specific active sites on the semiconductor's surface and exclude H_2 from the oxidation site and O_2 from the reduction site, shown in Figure 4. Once the primary photon absorption and electron

excitation processes have been realized in a semiconductor, for efficient OWS to yield green H_2, two different co-catalysts are loaded on the semiconductor surface to specifically trap the excited electron and holes, respectively. The co-catalysts that trap the electron, serves as a reduction site for proton reduction and promotes H_2 evolution. Whereas the other co-catalysts that traps the holes alone, serves as an oxidation reaction site on the semiconductor's surface and promotes O_2 evolution (Figure 4).

Table 1. State-of-the-Art Photocatalysts Loaded with H_2 and O_2 Evolution Co-catalysts for One-Step Photoexcitation Based OWS Process

S.No	*Photocatalysts*	*H_2 Evolution Co-catalysts*	*O_2 Evolution Co-catalysts*	*Reference*
1.	*InGaN/GaN Nanowires*	*Rh/Cr_2O_3 (Noble metal core/Chromium oxide shell)*	*Co_3O_4*	(*22*)
2.	*$Y_2Ti_2O_5S_2$*	*Rh/Cr_2O_3*	*IrO_2*	(*23*)
3.	*$SrTiO_3$:Al*	*$RhCrO_x$*	*CoO_y*	(*24*)
4.	*GaN:ZnO*	*Rh/Cr_2O_3*	*Mn_3O_4*	(*25*)
5.	*g-C_3N_4*	*Pt*	*CoO_x*	(*26*)
6.	*Si/TiO_2 nano-tree heterostructure*	*Pt*	*IrO_x*	(*27*)
7.	*$CaTaO_2N$*	*$RhCrO_y$*	*Ti-oxyhydroxide*	(*28*)
8.	*ZrO_2/TaON*	*RuO_x/Cr_2O_3*	*IrO_2*	(*29*)
9.	*P10(Homopolymer of dibenzo[b,d]thiophene sulfone)*	*Pd*	*Ir/IrO_2*	(*30*)
10.	*GaN:ZnO*	*Rh with decorated Al_2O_3*	-	(*31*)

As both the co-catalysts are loaded randomly on the photon absorbing single semiconductor surface, the entire system is termed as one-step photoexcitation path for the OWS-process. These co-catalysts primarily prevent the recombination of excited electrons and holes on the semiconductor's surface, introduces charge transfer selectivity, facilitates the facile transfer of charges. Subsequently, their other key function is to catalyze both the half reactions of OWS process by lowering their activation energies. Noble metals have been traditionally employed so far as the reduction co-catalysts. They act as electron sinks and their corresponding electron trapping ability stems from their work function property, which are greater than the work functions of semiconductors, employed for OWS-processes. The higher the work function of the metal, the lower its Fermi energy level. Hence, when a metal makes an intimate contact with the semiconductor, a Schottky-junction is formed (Figure 5). The equilibration of Fermi levels of both the metal and semiconductor occurs, resulting in the transfer of electrons from the semiconductor's conduction band to the metal. Among noble metals, platinum (Pt) possesses the largest work function, it experimentally disposes the lowest

Kumar; Towards Sustainable and Green Hydrogen Production by Photocatalysis: Scalability Opportunities and Challenges (Volume 1)
ACS Symposium Series; American Chemical Society: Washington, DC, 0.

activation energy for H_2 evolution (*32*). Due to such valuable characteristics, Pt exhibits the best electron trapping ability and serves as an excellent co-catalyst for H_2 evolution (*9*, *33*). The H_2 evolution on the reduction co-catalysts surface occurs through two diverse steps. The first step is called the discharge step, represented by equation (4) and the second and final step is called the catalytic step, shown by equation (5).

$$2H^+ + 2e^- \rightarrow 2[H_{ad}] \quad \textbf{(4)}$$

$$2[H_{ad}] \rightarrow H_{2(g)} \quad \textbf{(5)}$$

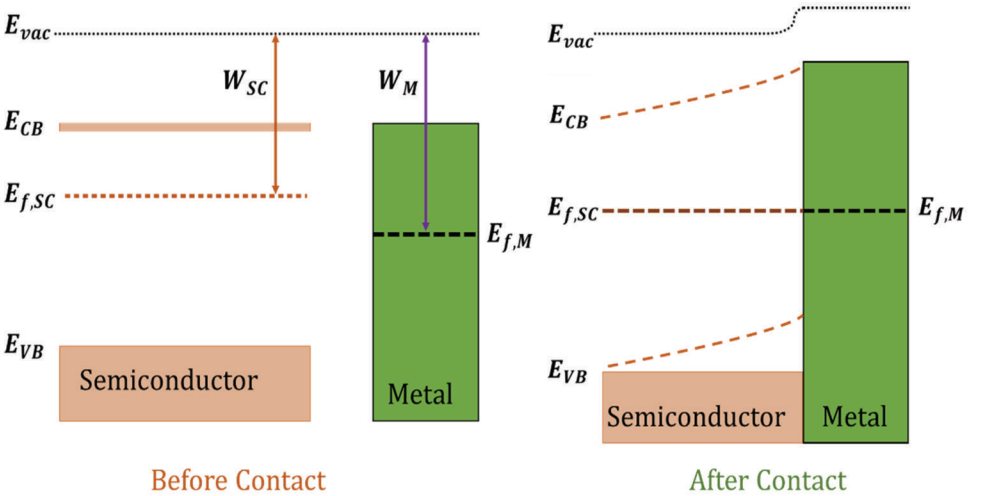

Figure 5. (a) Energy level positions in metal and semiconductor material before the formation of their heterojunction. (b) Schematic representation of the formation of Schottky junction upon the intimate contact of the semiconductor photocatalysts and metal-based reduction co-catalysts.

However, these noble metals (Pt, Pd, Rh, etc.) not only act as hydrogen evolution co-catalysts but also exhibits activity for the undesirable water formation reaction between the evolved H_2 and O_2 molecules and oxygen reduction reaction (ORR). To eliminate these backward reactions, the noble metal co-catalysts were coated with the Chromium (III) Oxide (Cr_2O_3) thin layer material, resulting in a core/shell structure. This Cr_2O_3 shell prevents the entry of the O_2 molecules to the noble metal core's surface where H_2 is evolving, on the contrary, it allows the hydrogen ions and reactant water molecules to reach the reduction co-catalysts. Thus, selective permeation enabled by the noble metal core/Cr_2O_3 shell systems prevents the happening of ORR and water formation reaction (*34*).

Complementarily, these Cr_2O_3 amorphous shells, along with maintaining the activity of noble metals as hydrogen evolution co-catalysts, it also subdue the detrimental effect on the photocatalytic activity by suppressing the augmenting background ambient pressure during the OWS process (*5*, *35*). Due to such beneficial characteristics, this shell system is being noticed in many recently reported photocatalysts performing OWS process though one-step photoexcitation technique, see entries (1,2,3, 4 and 8) in Table 1. In 2023, Li et al. (*31*) reported selective decoration of Aluminium Oxide (Al_2O_3) as reduction co-catalysts in Rh/GaN-ZnO photocatalytic system using atomic precision Atomic Layer Deposition (ALD) technique, alternative surface modification differing to the surface coverage provided by Cr_2O_3 shell system (entry 10 in Table 1). The selective decoration

prevented both the water formation and ORR reactions on the reduction co-catalysts surface, however it didn't suppress the diminishing effect on photocatalytic activity due to increasing background pressure during the OWS process. On the other hand, strikingly, this selective ALD Al_2O_3 decoration increased the Apparent Quantum Yield (AQE) of Rh/GaN-ZnO photocatalysts for OWS process from 0.3% to 7.1% at 420 nm (*31*) Additionally, Cui et al. (*36*) reported that spatioselective coating of Pt/Pd metals on the g-C_3N_4-based spheres, rendered self-propelling properties to the photocatalytic composite materials.

Like the H_2 evolution co-catalysts for water reduction half reaction, the O_2 evolution co-catalysts for water oxidation half reaction, is very crucial for photocatalytic systems targeting OWS-process. Cobalt Oxide (CoO_x) (*37*), Cobalt Phosphate (CoPi) (*37*), Ruthenium Oxide (RuO_x) (*38*), Iridium Oxide (IrO_x) (*39*, *40*), and Manganese Oxides (MnO_x) (*37*), are the various materials that promote O_2 evolution and serve as efficient co-catalysts for photocatalysts targeting water oxidation half reactions. Their modus operandi for achieving the specific charge transfer selectivity in the semiconductor photocatalyst surface, specifically for trapping the holes, can be explained by taking the metal-oxide (cobalt oxide) material as an example. The metal within this metal-oxide possesses variable valence state (Co has +2 and +4), Co metal facilely switches from +2 valence state to +4 valence state, when it traps the photogenerated holes on the semiconductor surface. In the end, it switches back to valence state +2 from +4, after oxidizing the water molecule and generating the O_2 gas molecules (*33*).

Finally, the overall photocatalytic system, loaded with both the reduction and oxidation co-catalysts on its surface can be technically visualized as a nano/micro-sized photoelectrochemical (PEC) cell studied for the overall water splitting process. Here, the reduction reaction occurring on the co-catalysts' sites can be seen as cathode and oxygen evolving co-catalysts' sites can be seen as an anode. The co-catalysts are pretty much equivalent to electrocatalysts loaded on the electrode surface, especially water oxidation co-catalysts. The photocatalytic performance of semiconductor-photocatalysts for OWS-process has been significantly enhanced upon the loading of oxidation co-catalysts on its surface, indicating that co-catalysts to great extent reduced the activation energy for the water splitting process. Even though in photocatalytic OWS-process, the required activation energy includes the energy needed for both half-cell reactions of water splitting process. As the water oxidation half-reaction is a passive, multi-step process involving the generation of four-proton and four-electron transfer process. Thus, the activation energy of water oxidation process influences the activation energy of overall OWS-process. The decrement in the activation energy upon the usage of oxidation co-catalysts, shown in Figure 6.

This can be experimentally seen in the case of PEC cell, where upon the loading of electrocatalysts on the photoanode surface (equivalent to oxidation co-catalysts on photocatalytic surface), the photocurrent has been greatly enhanced and there has been subsequent cathodic shift (negative shift) of the onset potential for water oxidation process. The negative shift of onset potential highlights that there has been a decrease in the overpotential associated with the process. This activation overpotential of PEC-cell studied for water splitting process is equivalent to the activation energy associated with photocatalytic process.

Having discussed the electrochemical benefits of co-catalysts in preventing indirect reactions of OWS-process and catalyzation of green H_2 and O_2 reactions through lowering of the activation energy. Note that the excessive loading of the co-catalysts does not increase the OWS-process. Most of the studies carried out so far, have realized co-catalysts loading amount around 0.1-2 wt% of the photocatalysts. The excessive loading of co-catalysts can shield the photons falling on the

photocatalytic surface, ultimately reducing the production of photo-excited electron and holes and leading to less quantity of green H_2 generation. Excessive loading of co-catalysts can also cover the other active sites present on the surface of photocatalysts reducing the intimate contact between the water molecules and the photocatalysts (*41*, *42*). Thus, for commercialization and large-scale implementation, simultaneous development of both photocatalysts and co-catalysts is important because the OWS-process is determined by the optimum balance existing between the rate of redox reaction of the co-catalysts surface and the rate of electron-hole generation on the photocatalytic material.

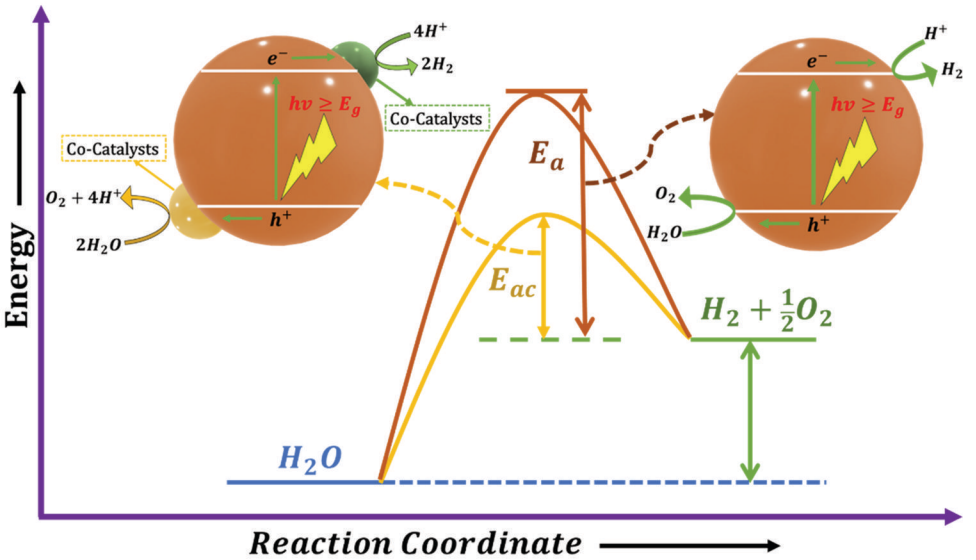

Figure 6. Schematic portrayal of the decrement of the activation energy upon loading of co-catalysts on the OWS photocatalysts employed in one-step photoexcitation process. Here 'E_a' corresponds to the activation energy required when unmodified semiconductor photocatalyst is employed. 'E_{ac}' corresponds to the activation energy required when co-catalyst(s) loaded photocatalytic-semiconductor is employed.

Effective Implementation of One-Step Photoexcitation Systems for Hydrogen Production

Hitherto, this chapter has been presented in the perspective of materials scientists, elucidating the fundamental insights about the requisites of the particulate photocatalysts for achieving the OWS-process. The performance of any photosystem implemented for green H_2 production using solar energy is compared and ranked based on the solar-to-hydrogen (STH) conversion efficiency. This parameter provides the facile comparison of reaction rates reported by several research groups, even though experimented in diverse settings (*43*). It is calculated using the equation (*6*).

$$STH(\%) = \left\{\frac{Energy\ of\ generated\ H_2}{Energy\ of\ incident\ solar\ light}\right\} * 100 \qquad (6)$$

There are three different solar-based photosystems employed for OWS process for green hydrogen production: (i) Photoelectrochemical cells, (ii) Photovoltaic (PV) coupled-electrolysis, and (iii) Heterogeneous Particulate Photocatalysis. Here, one-step photoexcitation and two-step photoexcitation subsystems fall within the particulate photocatalytic system. Despite the relatively

lower solar-to-hydrogen (STH) values observed in the currently studied particulate photocatalytic system, when compared to other photosystems harnessing solar energy for green hydrogen production, it remains a standout technology for future large-scale implementation. This prominence is primarily attributed to the cost-effectiveness associated with its fabrication and subsequent operation. For real-time testing (implementation) of one-step photoexcitation system, all it needs is a suspension of water containing the active photocatalytic (semiconductor loaded or coated with co-catalysts) materials exposed to solar light.

In laboratory conditions, the studies are conducted mostly using a Pyrex material-based flask type batch vessel, of 0.1–1 L volume (*43*). Generally, the photocatalyst material (for example: 0.1 g of photocatalysts in 300 mL of liquid volume) (*44*, *45*). is suspended using an intense magnetic stirring in the batch reactor. Such mechanical operations prevent the settling of the particulate photocatalysts at the bottom of the reactor. This suspension is exposed to either (simulated) sunlight or any other artificial light positioned either above or around the reactor. The generated gases are analyzed using gas chromatography (GC) (*44*). A part of reaction vessel is surrounded by a water jacket to maintain the temperature of the process (*44*). In order to achieve scalability of green H_2 production, direct scaling of the batch reactor system is practically non-feasible. As the cost of the reactor system becomes very high, and operation of such system requires giant magnetic stirrers, which further increases the operational and maintenance costs. As the volume of the photoreactor increases, the photocatalytic process becomes less efficient due to light attenuation effect with respect to the depth of the water (only 20% of photons belonging to the visible spectrum reaches to a water depth of 0.5 m) (*46*).

Practically, the future and the current researchers visualizing the scalability of green H_2 through particulate photocatalysis, should process enormous volumes of water, to provide the intimate contact between the semiconductor and photolyte. In the past, especially in the last decade, real-time study under natural sunlight exposure for large-scale green H_2 production was achieved by Jing et al. (*47*), by using sacrificial agents: Sodium Sulfite (Na_2SO_3) and Sodium Sulfide (Na_2S). The slurry suspension along with sacrificial agents was circulated in Pyrex-material made tubular reactor (total volume of reactor was 11.6 L and catalysts loading was 6.38 g of Cadmium Sulfide (CdS) powder) coupled to compound parabolic concentrator. Here, the average H_2 production rate was found to be 300 mL/h (*47*).

As soon as new semiconductor nanomaterial is developed for the OWS process. The precise determination of band edge positions or flat band edge potential of such new photocatalysts is not a facile task. If all the requisites of photocatalysts for OWS process are not met, no H_2 would be produced from water molecules under light exposure. Thus, H_2 generation capacity of any new-active photocatalysts can be tested by using irreversible electron donors in water. These molecules are termed as sacrificial agents, they specifically interact with the valence band (VB) holes upon photoexcitation, neutralizing them, thus promoting the charge separation of the photocatalysts for H_2 generation.

Heterogeneous photocatalytic H_2 generation from aqueous solutions in the presence of sacrificial agents or hole scavengers is not high endergonic process as the OWS splitting in the presence of photocatalysts alone. The standard Gibbs free energy (ΔG^o) for H_2 generation from water containing methanol as sacrificial agent is 9.3 kJ/mol (*48*). Still, even for this H_2 generation to occur, the VB edge of photocatalysts should be more positive than the oxidation potential of sacrificial agents (*9*, *49*). This process is not as challenging as the OWS process on heterogeneous

photocatalysts, as the electron-hole recombination is suppressed by hole scavengers and the reverse reaction of OWS process does not occur here, as the O_2 generation is avoided in this system. This process enables simultaneous generation of H_2 and photooxidation of sacrificial agents. This paves the way for the degradation (oxidation) of waste (for example biomass), which can be used as sacrificial agent, along with H_2 generation from water and this process can be termed as photo-reforming process (*20*).

However, the scaling up of photocatalytic reforming for green H_2 generation also faces similar challenges as the scale-up of OWS process based on one-step and two-step photoexcitation systems. In both cases, increasing the photocatalysts quantity does not increase the hydrogen evolution rate. For example, when the quantity of photocatalysts [Pt loaded composite of zirconium oxide/tantalum oxynitride (TaON)] was increased from 25 mg to 50 mg, the hydrogen evolution rate was decreased from 7.5 to 3.3 μmol/h, in the two-step photoexcitation system (*51*). The details and mechanistic understanding of two-step photoexcitation system will be described in detail in the upcoming section. In the photocatalytic system, with batch or continuous reaction vessels carrying the suspension of the photocatalyst, a decreasing production rate with increment of catalysts quantity could be primarily attributed to the light scattering phenomenon instead of enhanced light absorption by all the photocatalysts present in the system (*52*). At the same time, increment in volume of the photoreactor vessel will also lead to light attenuation (*46*), as previously discussed.

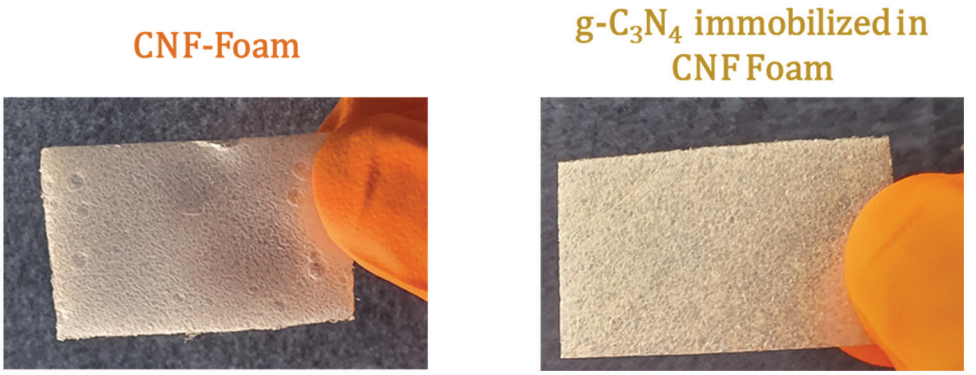

Figure 7. Photographs of Cellulose Nanofiber (NF)-based buoyant substrate material and g-C3N4 immobilized composite thin film floating photocatalytic material. These floating thin film photocatalysts were fabricated by Anusuyadevi et al. (46) Adapted with permission from reference (46). Copyright 2020 American Chemical Society.

Thus, for the scalable photocatalytic H_2 production to be practically feasible, any large-scale system proposed should ensure uniform absorption of photons by all the photocatalysts present in the system. Thus, for real-time implementation under natural solar irradiation, the above requirement can be facilely achieved in large scale by immobilizing/fixing the nano-photocatalytic powders on a substrate. As it provides the uniform utilization of photons and alleviates the complex recovery process of photocatalysts from the photoreactor. Drawing inspiration from thin film floating photocatalysts targeted in real-time pollutant removal using sunlight [graphitic-Carbon Nitride ($g\text{-}C_3N_4$)] photocatalysts in buoyant cellulose nanofiber foam (substrate), (Figure 7) (*53*) and solar cells, where the photon harvesting step is the crucial step as in photocatalytic process. Photocatalytic panels, fabricated in such a way that a uniform coating of semiconductor photocatalysts composites

(photocatalysts + co-catalysts) on thin film substrates (glass or metal), would be the ideal systems for scalability of green hydrogen production through photocatalysis.

To substantiate the above point of view, several works on photocatalytic powder immobilized panels were reported for the green H_2 generation. For instance, Gopinath et al. developed different panel-based thin film photocatalytic systems in lab scale for green hydrogen production from water containing methanol as sacrificial agent. The different photocatalysts studied by them as thin films coated on glass substrates by drop casting technique: 1) Commercial TiO_2 (P25) loaded with Pd co-catalysts (*52*), 2) Au-Pd/C/TiO_2 & Au-Pd/rGO/TiO_2 (*54*), 3) Bimetallic Cu-Ni deposited TiO_2 (*55*), and 4) Ag loaded TiO_2 (*56*).

Scalability Studies of One-Step Photoexcitation System through Thin Film Photocatalysis for Green Hydrogen Production

In the regime of up-scaling of thin film photocatalysis for green H_2 , Schroder et al. (*57*). reported a large scale photoreactor, where platinum (Pt) loaded mesoporous g-C_3N_4 was immobilized on nine stainless steel plates (each plate was 3.5 cm*3.5 cm*0.25 cm) by drop-coating technique, by using Nafion as a polymeric binder. These plates were placed inside a photoreaction chamber, whose bottom side was made up of Teflon plate (28 cm *30 cm *0.1 cm). Above the stainless-steel substrates, the top of the photoreactor is closed with plexiglass window, see Figure 8. Here 18 L of hydrogen was produced within a month, by exposing the above photoreactor to natural sunlight from the aqueous solution containing 10 vol% of triethanolamine, which was used as sacrificial agent. The total volume of the aqueous solution was 10 L, and it was kept under circulation using a pump (*57*).

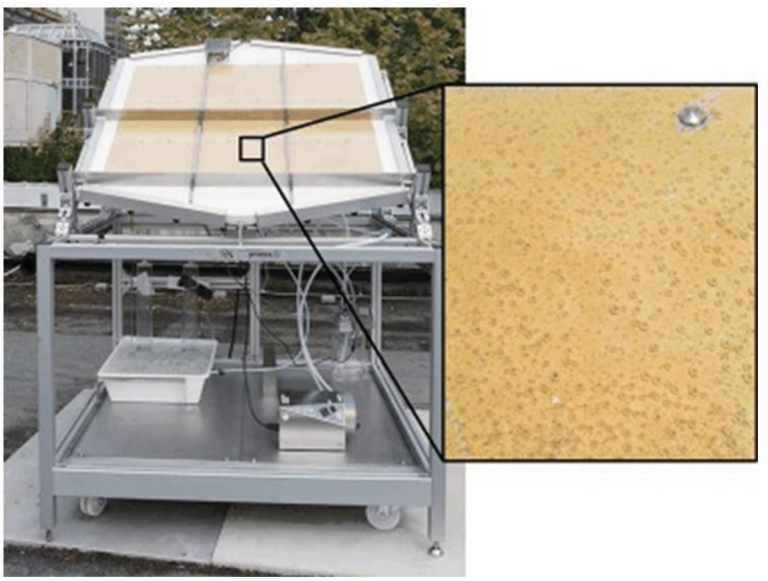

Figure 8. Photograph of a large scale photoreactor, reported by Schroder et al., working under natural sunlight conditions (*57*). *The zoomed image shows the hydrogen bubbles occurring on the surface of the immobilized g-C_3N_4 photocatalysts under OWS process. Adapted with permission from reference* (*57*). *Copyright John Wiley & Sons.*

Kumar; Towards Sustainable and Green Hydrogen Production by Photocatalysis: Scalability Opportunities and Challenges (Volume 1)
ACS Symposium Series; American Chemical Society: Washington, DC, 0.

Recently, Goto et al. (*24*) reported a large-scale flat panel reactor with a light exposure area of 1 m^2. They were successful in carrying out OWS process to produce H_2 and O_2 from distilled water without sacrificial agents. The photocatalysts employed here for one-step photoexcitation, realizing OWS-process was Aluminium (Al) doped Strontium Titanate ($SrTiO_3$). This semiconductor photocatalyst was loaded with Rhodium-Chromium mixed oxide ($RhCrO_x$) as the co-catalysts and finally co-loaded with Cobalt Oxide (CoO_y). The 20 mg of Al-$SrTiO_3$ powder photocatalysts was mixed with 40 mg of silica nanoparticles with 400 μL of distilled water. Subsequently, the mixture was ultrasonicated, drop casted on frosted glass plate (33 cm*33 cm), finally heated on a hot plate at 50 °C. The above process of drop coating was repeated ten times and finally, the plate was heated at 623 K for 1 h in air (*24*). Finally, nine of these glass plates were arrayed in 1 m^2 panel type reactor. This panel was pretty much identical to the panel reported by Schroder et al. (*57*), see Figure 8.

Under exposure to natural sunlight conditions, the above $SrTiO_3$-Al based photocatalytic panel released 508 mL of H_2 during the first 30 min of the OWS process (*24*). Precise control of porosity and hydrophilicity of the photocatalytic powders' coating, retains the enhanced photocatalyst activity of the semiconductor material. On the other hand, densely packed photocatalytic layers display very low H_2 activity, as the diffusion of water molecules and desorption of gas molecules are very difficult to be achieved from dense packing of the semiconductor materials. These problems are alleviated by adding hydrophilic silica particles along with photocatalytic powder suspension during the coating process. Silica particles create voids among the coated packing of photocatalytic materials, which facilities facile diffusion of water molecules and desorption of gas molecules from the coated photocatalytic materials. This explains the motivation for the addition of silica particles along with particulate photocatalysts during the fabrication of panel rectors (*58*).

Following the 1 m^2 panel photoreactor system, Hiroshi et al. (*59*) reported a scaled-up and safe operation of 100 m^2 panel reactors with modified photocatalysts based on the work of Goto et al. (*24*) This large-scale system was realized using 1600 small-sized reactor sheets/units. Here, each unit has a light exposure area of 25 cm*25 cm, as shown in Figure 9a. Here, the distance between the glass window and the photocatalytic sheet is adjusted to 100 μm to obtain the optimal water load thus, limiting the augmentation and ignition of the generated gas (H_2 and O_2) molecules, see Figure 9b. Finally, the complete overview picture of 100 m^2 particulate panel system consisting of 1600 units is shown in Figure 9c. Here, the H_2 separation from the moist gas mixture was realized through commercial polyimide membrane, the gas separation unit using these membranes, is shown within the yellow box in Figure 9c. To conclude, the system in Figure 9 is the largest particulate photocatalytic system for OWS process, reported so far using the one-step photoexcitation step. However, the photocatalysts employed here absorb light in ultra-violet region and under natural solar irradiation exhibit a STH conversion efficiency of 0.76%. Even though the current scalability studies demonstrate the hazard-free, large scale water splitting process with facile gas-collection and separation. The futuristic commercialization of one-step photoexcitation system for OWS process will be possible only when we achieve STH in the range of 5-10% and durability of the photocatalytic sheets of about 10 years. Thus, the three key factors to be addressed in the forthcoming days are: 1) Increment of STH efficiency, 2) Photocatalyst stability and durability, and 3) Facile gas collection and separation facility.

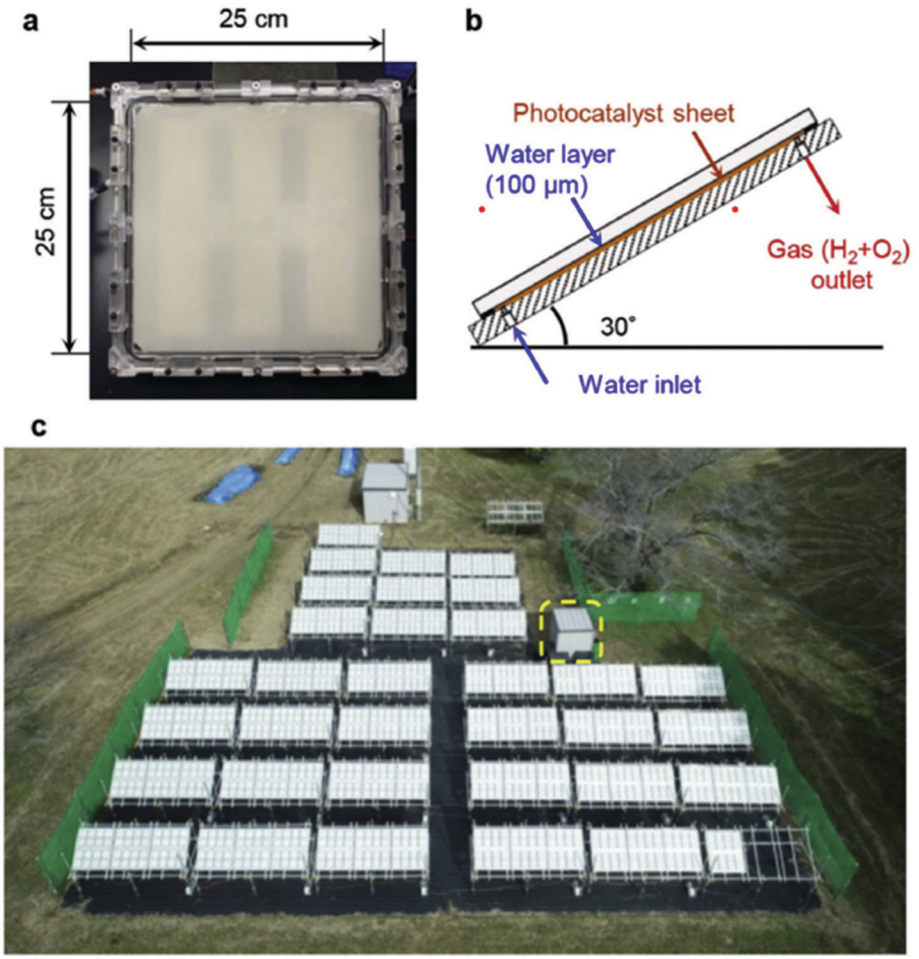

Figure 9. Scalable solar water splitting demonstration using Al:$SrTiO_3$ photocatalysts with a 100 m^2 array of panel reactor. (a) Photograph of single unit in panel reactor with a light exposure irradiation of 625 cm^2 (b) Cross-sectional view of reactor unit within the panel system, displaying the distance between the photocatalytic sheet and the glass window (c) Overview photograph of 100 m^2 array of panel reactor consisting of 1600 reactor units. Adapted with permission from reference (60). Copyright 2022 Elsevier.

The one step photoexcitation system, owing to its simplicity, can be scaled up efficiently for green hydrogen production by employing single semiconductor. However, this semiconductor material must meet the thermodynamic feasibility and achieve OWS process while retaining the photostability. To be specific, the semiconductor photocatalysts' conduction band (CB) minimum energy level and reduction-based decomposition potential should be more negative than the potential required for the proton to hydrogen conversion [$(E_{H^+/H_2} = 0\ eV\ vs\ NHE)$, at pH=0]. At the same time, the valence band (VB) maximum energy level should be more positive than both the oxidation-based decomposition potential and oxidative potential for O_2 generation [oxidation potential of H_2O to O_2 $(E_{O_2/H_2O)} = 1.23\ eV\ vs\ NHE)$, at pH=0] (5). This restricts the use of semiconductor photocatalysts with band gap active in the far visible and near IR regions of the solar spectrum. Interestingly, the STH conversion efficiency increases only when we attempt to use

photons from longer wavelengths of the solar spectrum. See the STH vs photon wavelength graph in Figure 10.

Another engineering requirement posed by the one-step photocatalytic system is the need for additional equipment to separate the explosive H_2-O_2 mixture. This further escalates the cost of hydrogen production. Thus, to increase the STH conversion efficiency by alleviating the thermodynamic requirement and elimination of the separation cost, two-step photoexcitation system was parallelly studied in the photocatalytic water splitting field along with one-step photoexcitation system.

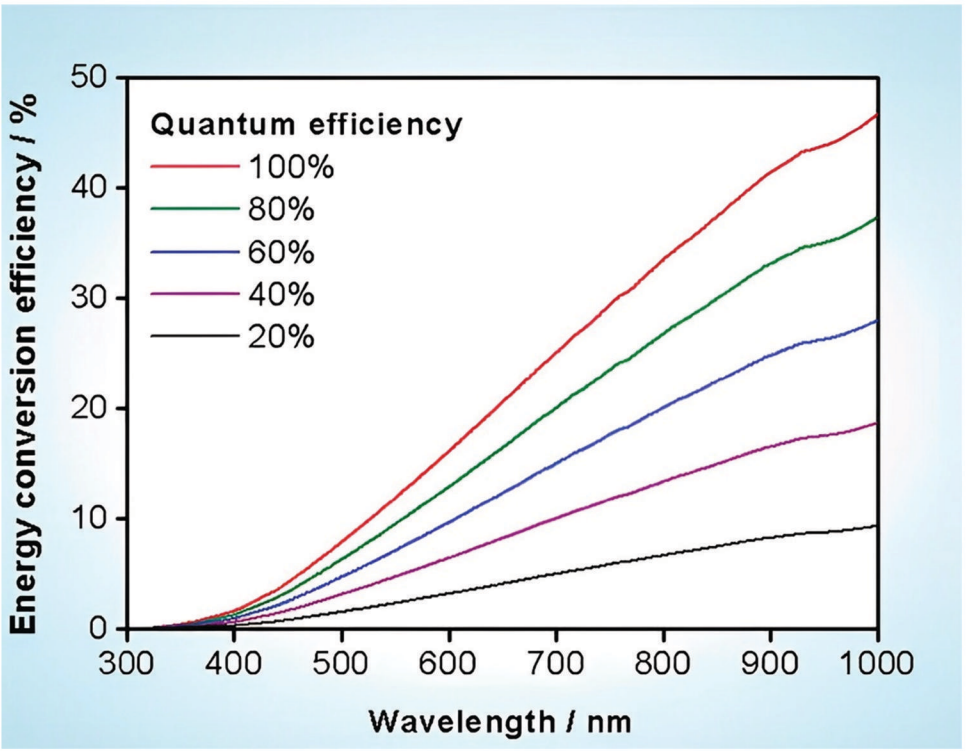

Figure 10. Estimated STH conversion efficiency as a function of wavelength of photon used for hydrogen generation using the one-step photoexcitation system. Estimation done here are achieved by employing solar irradiance of Air Mass (AM) 1.5. Reproduced with permission from reference (*42*). *Copyright 2010 American Chemical Society.*

Two-Step Photoexcitation System for Photocatalytic Green Hydrogen Production

Nature is the biggest inspiration for harnessing the solar energy and converting it into a usable chemical energy. For instance, during photosynthesis, green plants absorb sunlight, split water molecules to produce O_2 and protons. Here, O_2 is released into the atmosphere, whereas the protons are coupled with CO_2, subsequently reduced to valuable chemicals (for example: carbohydrates). Here both the oxidation and reduction half-cell reactions are spatially separated from each other (*60*, *61*). Inspired by this, the Z-scheme system was developed. it is a dual-photocatalytic system consisting of a hydrogen evolution photocatalyst (HEP) and an oxygen evolution photocatalyst (OEP), which are spatially separated to perform water reduction and oxidation reactions, respectively. OEP oxidizes water to oxygen via holes, whereas HEP generates H_2 via the photoexcited

electrons of the HEP semiconductor material, see Figure 11. The recombination of holes of HEP and electrons of OEP occurs through a pair of reversible redox mediators that form the charge neutralization path (*49*). The redox couple is chosen in such a way that it selectively interacts with photocatalysts inhibiting backward reactions, thus facilitating the spatial separation of H_2 and O_2 evolution reactions.

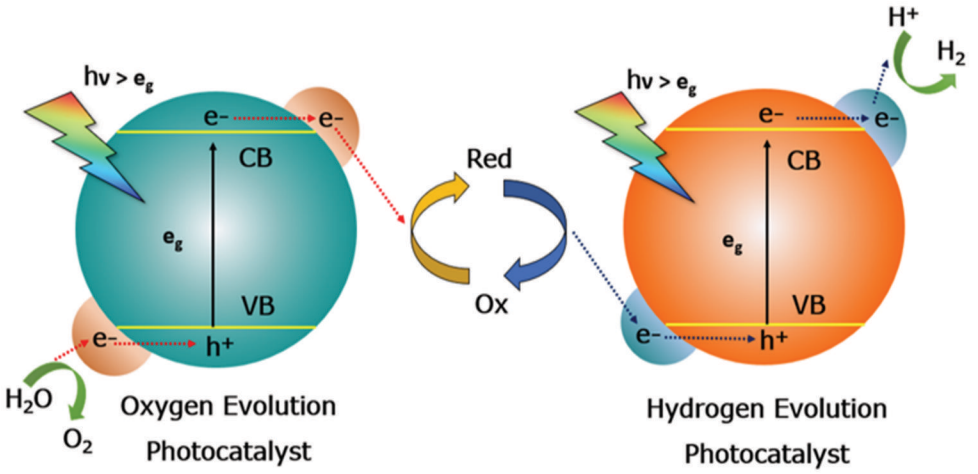

Figure 11. Schematic representation of the two-step photoexcitation system for the OWS process.

The two-step photoexcitation system is highly beneficial as it enables us to use narrow band gap (visible light active) semiconductor materials as HEP and OEP. As the band gap of the semiconductor does not need to straddle both the oxidation and reduction potential of water. However, the CB minimum energy level of HEP should be more negative than the reduction potential of water, simultaneously, the VB maximum of OEP should be more positive than the oxidation potential of water (*49*). These narrow band gap HEP and OEP semiconductors are still loaded with co-catalysts to prevent light induced photodecomposition (photo-corrosion) of the semiconductor and to achieve the required charge transfer selectivity as explained in the one-step photoexcitation system.

Even though, the two-step system removes the strict thermodynamic requirements of the one-step photoexcitation-based single semiconductor material, unlike the later system, it requires eight electrons for the O_2 generation and four electrons for the H_2 generation. Due to this, the quantity of H_2 and O_2 produced in the Z-scheme is equivalent to half of the quantity produced from the one-step process. This points out that to achieve a similar STH value, twice the quantum yield (QE) is necessary for the Z-scheme system in comparison to the one-step photoexcitation process. Thus, to conclude, the two-step photoexcitation system expands the spectrum of choosing a wide range of narrow band gap semiconductors, due to the removal of thermodynamic requirements, but kinetically it is a more challenging process than the one-step technique. As the number of elementary steps is higher, due to the interparticle charge transfer occurring between the HEP and OEP through redox mediators.

Scalability Trails for Z-Scheme System

A dual-compartment particulate suspension reactor assembly has been reported to scale up the Z-scheme system. The photolytic suspension of HEP and OEP are localized separately in two

Kumar; Towards Sustainable and Green Hydrogen Production by Photocatalysis: Scalability Opportunities and Challenges (Volume 1)
ACS Symposium Series; American Chemical Society: Washington, DC, 0.

different compartments covered with a transparent plastic film (baggies) to contain the gas generated. These beds are connected by fabric mat barriers that are permissible to redox ions but not to the gas generated (*62*). A conceptual pilot plant setup has been reported, where they utilized the baggie reactor system to synthesize 1000 kg of hydrogen per day with a photo capture area of 126969 m^2 and estimated land utilization of 165060 m^2, having an STH of 5% (*63*). These theoretical evaluations proved critical in designing the experiments, assimilating the underlying phenomenon and optimizing the experimental conditions. The large area requirements have prompted the researchers to develop a tandem reactor setup. As illustrated in Figure 12, O_2 evolution and reduction of shuttle ion occurs in the top compartment. The reduced shuttle ions and protons then diffuse through the porous bridge into the tandem compartment, where the evolved H_2 is collected in the polymer-based collection unit. Stacking these chambers enable effective mass transfer over short distances, enabling continuous operation without the need for external convection (*64*, *65*).

However, due to the complexities associated with this design and the bulkiness of the system coupled with low STH (5%), the commercial realization of the baggie system in the near future is uncertain. An elaborate pumping system will be required to keep the suspension from aggregation, the operation of the system comes to a halt as soon as photocatalyst sediments. Moreover, the limitations of conduction and valance band potential, light diffusion and migration of ions across the perforated bridges reduce the scalability of this system. Furthermore, if not adequately monitored, this system accumulates transparent hydrogen gas, which raises safety concerns and calls into doubt its viability. Therefore, to pave the way for the safe scalability of H_2 production, Sayama et al. (*66*) proposed a photocatalysis and electrolysis coupled hybrid system.

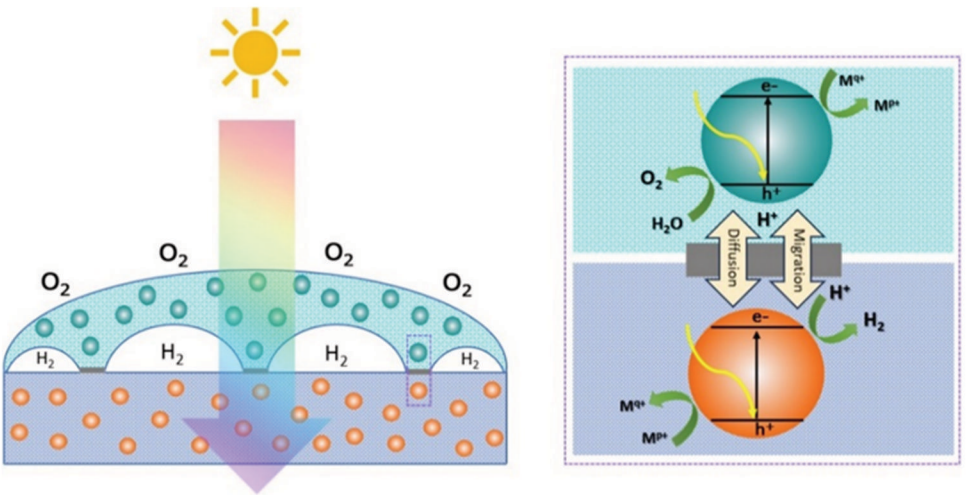

Figure 12. The image on the left schematically represents the green hydrogen production system using a dual bed reactor system. The image on the right provides an in-depth view of the localization of HEP and OEP semiconductor materials of Z-scheme system.

Scalable Green Hydrogen Production via the Hydrogen Farm Project (HFP)

Drawing parallels from the above Z-Scheme system, another scalable photocatalytic green hydrogen production system has been developed, which is widely referred to as a solar hydrogen farm project, schematically illustrated in Figure 13. It is operated by employing particulate OEP semiconductor material alone, suspended in a reaction pool to absorb solar energy. This generates

O_2 and protons in the presence of sunlight irradiation, simultaneously reducing the shuttle ions. The protons and reduced shuttle ions are then transferred to the electrolyzer, where protons are simultaneously reduced to H_2 on the cathode side and the shuttle ions are oxidized on the anode side which are pumped back to the photocatalytic pool (*67*).

The choice of redox mediator largely depends on the voltage required for the reduction of the ions. Conventional hydrolysis requires a high voltage of 1.8 V–2.6 V (*68*). Therefore, to reduce the cost it is economical to choose a redox mediator pair whose reduction potential is below the given range to make the process commercially feasible. The reduction potential of Fe^{2+}/Fe^{3+} is 0.77 V, and I_3^-/I^- is 0.545 V, making such redox mediators a good choice for this system. The most widely used OEP to realize HFP is $BiVO_4$ with a Fe^{2+}/Fe^{3+} redox couple. The photo stability of $BiVO_4$ is increased by facet engineering (*69*).

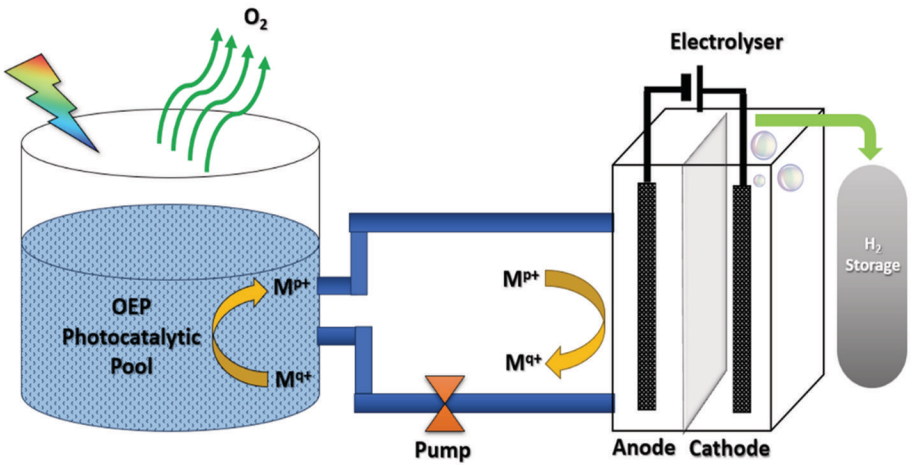

Figure 13. Schematic representation of the solar hydrogen farm project (HFP).

The apparent quantum efficiency (AQE) for photocatalytic water oxidation can be optimized to over 71% in the presence of Fe^{3+} ions as electron acceptor, by precisely tuning the exposed {110} and {010} facets of $BiVO_4$ crystals, while the reverse reaction, from Fe^{2+} to Fe^{3+}, was completely blocked (*67*). A panel-type reactor is suggestable to scale up this system to avoid the complexities arising from the suspension photocatalytic pool. The other half reaction of OWS process occurs in the electrolyzer, where H^+ is reduced to H_2. This automated setup is experimentally demonstrated by Li et al. (*70*), where the reaction solution was pumped into the reactor using a peristaltic pump, entering from a bottom inlet and exiting from a top outlet. He reported that this circular flow of the reaction solution effectively minimized the impact of mass transport effects. Upon the complete conversion of all Fe^{3+} ions into Fe^{2+} ions, the reaction solution was subsequently transferred to the electrolysis cell for hydrogen production. The design incorporated a tilt of the reaction plate, allowing continuous adjustment from 0° to 30°, facilitating optimal absorption of sunlight for the process (*70*).

We propose a concept of alternating units of tandem oxygen evolution photocatalytic sheet with thin film electrolyzers and a solar cell unit (to power the electrolyzer) in a panel to make a compact and clean HFP system. The photocatalytic sheets can be fabricated using the screen printing

technique (*35*). We anticipate that in the future these photocatalytic sheets could be potentially fabricated using the atomic layer deposition (ALD) technique.

Future Outlook

Techno-economic analysis reveals that particulate photocatalytic system is more economical and the most flexible in terms of infrastructure, exhibiting the highest propensity for scalability. However, significant research is required to improve the STH to at least 10% to compete with the existing systems. Limitations hindering the scalability have been identified as 1) Mass transfer limitations, 2) Low STH, and 3) Stability and photo-corrosion.

Reactors to Enhance Mass Transfer

It becomes vital to use new reactor designs and combinations to enhance mass transfer. Other than the plate-type reactor discussed in the HFP section, optofluidic microreactors gained the interest of the researchers to address this mass transfer inadequacy, as Z-scheme systems are mass transfer limited. Scaling up of the microreactor system can be done by numbering up the microreactors. Experimental studies were carried out using redox reactions mediated by iodide/iodate (I^-/IO_3^-) pairs which are employed to characterize the water-splitting reactions on the Pt/TiO_2 catalysts (*71*, *72*). Recycle studies were conducted on the photocatalytic films in the microreactor to check its durability. It was found that, an IrO_2/TiO_2 film could withstand 4 cycles of 5 h each during the water splitting process in the presence of sacrificial agents. This shows that the films had a strong bonding to the glass substrate, which is necessary for the long-term operation of the planar microreactor (*73*). Nevertheless, further research is necessary to attain the scalability of hydrogen production using this microreactor system employing single-photoexcitation technique for OWS process.

Despite making mass transfer advancements in the reactor systems, the complex and bulky infrastructure limits the scalability of Z-scheme/HFP systems. The continuous contact of the photocatalyst with the electrolytic/ionic solution causes corrosion of the catalyst forcing its replacement within a short period, making these systems uneconomical for scalability. Hence, improving STH and the photostability of the photocatalysts employed in the simple one-step photoexcitation system would be the most feasible option.

Enhancement of STH

There are several factors that limit the STH efficiency of a photocatalyst system (photocatalysts co-loaded with H_2 and O_2 evolution co-catalysts). Light-absorption range of the semiconductor photocatalysts, recombination rate of excited charge carriers, catalytic surface area, undesirable side reactions, augmentation of pressure of the photoreactor during OWS process, etc. Amongst which, the light absorption range determines the theoretical maximum of STH efficiency. In the one-step photoexcitation for OWS process, if any photocatalysts exhibits the propensity to absorb longer range wavelength of the solar spectrum and still possess the thermodynamic requirements for H_2 generation (appropriate position of CB and VB) can deliver higher STH efficiency, see Figure 10.

Interestingly, Zhou et al. (*22*) employed visible light responsive (400-700 nm) InGaN/GaN nanowire photocatalysts, coloaded with Rh/Cr_2O_3 and Co_3O_4, H_2 and O_2 evolution co-catalysts and achieved STH in the range of 2-3%. Strikingly, they combined photothermal effect (heating

Kumar; Towards Sustainable and Green Hydrogen Production by Photocatalysis: Scalability Opportunities and Challenges (Volume 1)
ACS Symposium Series; American Chemical Society: Washington, DC, 0.

achieved by making use of infrared (IR) light of solar spectrum) with one-step photoexcitation based OWS process and delivered a very high STH of 9.2%. Their photoreactor system was fitted with a heat insulation layer system to make use of the IR rays to reach and to maintain a temperature of about 70 °C. However, without the heat-insulation, the STH efficiency of the system drops down to 2-3%, as the photoreactor temperature falls to 50.8 °C. The enhanced STH efficiency is attributed to the dependency of the H_2 and O_2 recombination backward reaction. The higher temperature favoured the forward reaction of water splitting and inhibited the water formation reaction. However, their enhanced STH efficiency of 9.2% declined after 74 h of continuous OWS process, specifically attributed to the partial deactivation of the photocatalysts system due to the loss/decrement of co-catalysts materials (*22*).

Another alternative synergistic strategy, currently addressed is to combine the photocatalytic system used in one step photoexcitation with bigger sized (120-160 nm) plasmonic metal nanoparticles to render the photocatalytic system responsive to longer wavelengths in the solar spectrum (up to 850 nm), enabling to achieve STH around 7.6% (*74*). However persistent fundamental studies have to be continued in this synergistic regime to ensure the STH efficiency is maintained after continuous OWS process for scalable green hydrogen production.

Improving the Photostability of the Photocatalyst

Any semiconductor targeted for scalability in one-step or two-step photocatalytic system should potentially exhibit enhanced photostability (to achieve a lifetime of 10 years) and STH in the range of 5–10%. So far much lab scale study carried out, focused a lot on achieving high STH, whereas negligible attention was provided for studying the photo-induced decomposition of the semiconductor (photo-corrosion) and the co-catalysts nanoparticles. This negligence has precluded the scalability of photocatalytic systems for green hydrogen production. Limitation of photo-corrosion with enhanced STH can be a potential breakthrough to achieve commercial scalability of green hydrogen production using one-step photoexcitation system. Majorly, it has been identified that photo-corrosion occurs due to hole-induced photoinstability (*75*). It has been observed that transfer of photogenerated holes unlike electrons is rather complex. So, these holes reside on the photocatalyst surface, oxidize the metal surface, before reacting with a redox pair, thus the photocatalyst undergoes corrosion causing instability (*76*). This is mostly seen in metal-sulfide (CdS) photocatalysts. CdS is economical and shows exceptional efficiency as photocatalyst, however, the photocatalytic application of CdS is currently restricted due to its photo instability caused by holes as annotated in equations 7, 8, and 9. We can see that S^{2-} oxidizes to S^0, see equation 8, or to sulphate (SO_4^{2-}) as annotated by equation 9, depending on the availability of the O_2.

$$CdS \xrightarrow{h\nu} e^- + h^+ \quad \textbf{(7)}$$

$$CdS + 2h^+ \rightarrow Cd^{2+} + S \quad \textbf{(8)}$$

$$CdS + 2O_2 \rightarrow Cd^{2+} + SO_4^{2-} \quad \textbf{(9)}$$

Photo-corrosion was observed in metal oxide photocatalysts as well, where the photocatalyst decomposes (ZnO decomposes to Zn^{2+} and O_2) (*77*) or changes to a different oxidation state (Cu_2O becomes CuO) (*78*). Inhibition of this photo-corrosion can be addressed by removing either oxygen or photogenerated holes from the system. Removal of O_2 is facilitated by compounds like perfluoro

Kumar; Towards Sustainable and Green Hydrogen Production by Photocatalysis: Scalability Opportunities and Challenges (Volume 1)
ACS Symposium Series; American Chemical Society: Washington, DC, 0.

decalin (PFDL) and hemin chloride which are chemically inert, stable oxygen carriers (*79*). Due to the usage of such compounds, oxygen is moved away from the surface of CdS, preventing the O_2-induced photo-corrosion, thereby successfully suppressing the backward reaction of water splitting. Another way to address photo-corrosion is to isolate holes by having a protection layer over CdS sites. Chromium oxide (Cr_2O_3) reportedly realizes this function and shows excellent co-catalyst properties (*42*, *79*). Care was taken that when the CdS particles were coated with Cr_2O_3 particles, there is good interfacial contact so as to increase the photocatalytic activity. The Cr_2O_3 shell was homogeneously coated on the surface of CdS/Pt core, forming a coaxial heterostructure, delivering a high hydrogen evolution rate without any requirement of a sacrificial donor (*80*). Here, PFDL was used to remove nascent oxygen and the system did not show any instability, thus making it a viable option for scalability in the near future. Even though, the photocatalysts and/or reduction co-catalysts were coated with protective Cr_2O_3 amorphous coating, after continuous operation for several days, the deactivation of the photocatalysts starts to occur due to the loss of co-catalysts molecules. Thus, more fundamental research is required to realize the benefits of such protective coatings. Importantly, this Cr_2O_3 coating not only prevents photo corrosion, but it also suppresses the undesirable water formation reactions, to a major extent subduing the deactivation of photocatalysts due to the increase of ambient pressure during OWS process. Such in-depth insights will help us to realize more novel materials in the future with higher performance and facile synthesis steps for producing these materials on a large-scale for real-time implementation of green H_2 production.

Conclusions

One-step and two-step photoexcitation systems for OWS process are fundamentally described in this work. To conclude one-step photoexcitation system is the most tangible options for effective enforcement of scalable green hydrogen production. One-Step Photoexcitation is thermodynamically stringent, while two-step photoexcitation is kinetically restricted. Nevertheless, the commercial realization of one-step photoexcitation system can be achieved using various technologies, out of which panel type thin film reactor systems have a high potential for propelling extensive implementation of green hydrogen production. However, it may be noted that there are several factors that limit its commercial scalability: 1) Low STH, 2) stability of photocatalysts under long term operation, and 3) development of large-scale production methods of immobilized photocatalytic panels. To alleviate these limitations, immense efforts are required from research communities of diverse fields (material science, chemical engineering, etc.) to achieve large scale commercial production of green hydrogen through heterogeneous photocatalysis.

References

1. Anusuyadevi, P. R.; Kumar, D. J. P.; Jyothi, A. D. H. V. O.; Patwardhan, N. S.; V, J.; Mol, A. Towards Viable Eco-Friendly Local Treatment of Blackwater in Sparsely Populated Regions. *Water (Switzerland)* **2023**, *15*, 542. https://doi.org/10.3390/w15030542.
2. Singh, L.; Wahid, Z. A. Methods for Enhancing Bio-Hydrogen Production from Biological Process: A Review. *Journal of Industrial and Engineering Chemistry* **2015**, *21*, 70–80. https://doi.org/10.1016/j.jiec.2014.05.035.

3. Kim, J. H.; Hansora, D.; Sharma, P.; Jang, J. W.; Lee, J. S. Toward Practical Solar Hydrogen Production-an Artificial Photosynthetic Leaf-to-Farm Challenge. *Chemical Society Reviews* **2019**, *48*, 1908–1971. https://doi.org/10.1039/c8cs00699g.
4. Armaroli, N.; Balzani, V. The Hydrogen Issue. *ChemSusChem* **2011**, *4*, 21–36. https://doi.org/10.1002/cssc.201000182.
5. Wang, Q.; Domen, K. Particulate Photocatalysts for Light-Driven Water Splitting: Mechanisms, Challenges, and Design Strategies. *Chemical Reviews* **2020**, *120*, 919–985. https://doi.org/10.1021/acs.chemrev.9b00201.
6. Velazquez Abad, A.; Dodds, P. E. Green Hydrogen Characterisation Initiatives: Definitions, Standards, Guarantees of Origin, and Challenges. *Energy Policy* **2020**, *138*. https://doi.org/10.1016/j.enpol.2020.111300.
7. Sen, R.; Das, S.; Nath, A.; Maharana, P.; Kar, P.; Verpoort, F.; Liang, P.; Roy, S. Electrocatalytic Water Oxidation: An Overview With an Example of Translation From Lab to Market. *Frontiers in Chemistry* **2022**, *10*. https://doi.org/10.3389/fchem.2022.861604.
8. Bowker, M. Sustainable Hydrogen Production by the Application of Ambient Temperature Photocatalysis. *Green Chemistry* **2011**, *13*, 2235–2246. https://doi.org/10.1039/c1gc00022e.
9. Clarizia, L.; Russo, D.; Di Somma, I.; Andreozzi, R.; Marotta, R. Hydrogen Generation through Solar Photocatalytic Processes: A Review of the Configuration and the Properties of Effective Metal-Based Semiconductor Nanomaterials. *Energies* **2017**, *10*, 1624. https://doi.org/10.3390/en10101624.
10. Hota, P.; Das, A.; Maiti, D. K. A Short Review on Generation of Green Fuel Hydrogen through Water Splitting. *International Journal of Hydrogen Energy* **2023**, *28*, 523–541. https://doi.org/10.1016/j.ijhydene.2022.09.264.
11. Gupta, A.; Likozar, B.; Jana, R.; Chanu, W. C.; Singh, M. K. A Review of Hydrogen Production Processes by Photocatalytic Water Splitting – From Atomistic Catalysis Design to Optimal Reactor Engineering. *Int J Hydrogen Energy* **2022**, *47*, 33282–33307. https://doi.org/10.1016/j.ijhydene.2022.07.210.
12. Kumar, P.; Kumar, A.; Joshi, C.; Boukherroub, R.; Jain, S. L. Graphene-Semiconductor Hybrid Photocatalysts and Their Application in Solar Fuel Production. In *Advanced 2D Materials*; Wiley, 2016; pp 353–386. https://doi.org/10.1002/9781119242635.ch9.
13. Kozlova, E. A.; Parmon, V. N. Heterogeneous Semiconductor Photocatalysts for Hydrogen Production from Aqueous Solutions of Electron Donors. *Russian Chemical Reviews* **2017**, *86*, 870–906. https://doi.org/10.1070/rcr4739.
14. *Designation: E490 – 22 Standard Solar Constant and Zero Air Mass Solar Spectral Irradiance Tables 1*. https://doi.org/10.1520/E0490-22.
15. *Designation: G173-23 Standard Tables for Reference Solar Spectral Irradiances: Direct Normal and Hemispherical on 37° Tilted Surface 1*. https://doi.org/10.1520/G0173-23.
16. Maeda, K.; Takata, T.; Hara, M.; Saito, N.; Inoue, Y.; Kobayashi, H.; Domen, K. GaN:ZnO Solid Solution as a Photocatalyst for Visible-Light-Driven Overall Water Splitting. *J Am Chem Soc* **2005**, *127*, 8286–8287. https://doi.org/10.1021/ja0518777.
17. Kibria, M. G.; Nguyen, H. P. T.; Cui, K.; Zhao, S.; Liu, D.; Guo, H.; Trudeau, M. L.; Paradis, S.; Hakima, A. R.; Mi, Z. One-Step Overall Water Splitting under Visible Light Using

Multiband InGaN/GaN Nanowire Heterostructures. *ACS Nano* **2013**, *7*, 7886–7893. https://doi.org/10.1021/nn4028823.

18. Takasugi, S.; Tomita, K.; Iwaoka, M.; Kato, H.; Kakihana, M. The Hydrothermal and Solvothermal Synthesis of LiTaO3 Photocatalyst: Suppressing the Deterioration of the Water Splitting Activity without Using a Cocatalyst. *Int J Hydrogen Energy* **2015**, *40*, 5638–5643. https://doi.org/10.1016/j.ijhydene.2015.02.121.
19. Anusuyadevi, P. R. *Synthesis of Novel Nanophotocatalyst in Millifluidic Supercritical Reactor*. Doctoral Thesis, ICMCB - Institut de Chimie de la Matière Condensée de Bordeaux, Bordeaux, 2018. https://theses.hal.science/tel-02170508 (accessed 2024-02-22).
20. Osterloh, F. E. Photocatalysis versus Photosynthesis: A Sensitivity Analysis of Devices for Solar Energy Conversion and Chemical Transformations. *ACS Energy Letters* **2017**, *2*, 445–453. https://doi.org/10.1021/acsenergylett.6b00665.
21. Anusuyadevi, P. R.; Campbell, Z. S.; Erriguible, A.; Marre, S.; Aymonier, C. Supercritical Millifluidic Reactor for the Synthesis of Efficient GaN Nanophotocatalysts. *Chemical Engineering Journal Advances* **2023**, *14*. https://doi.org/10.1016/j.ceja.2023.100483.
22. Zhou, P.; Navid, I. A.; Ma, Y.; Xiao, Y.; Wang, P.; Ye, Z.; Zhou, B.; Sun, K.; Mi, Z. Solar-to-Hydrogen Efficiency of More than 9% in Photocatalytic Water Splitting. *Nature* **2023**, *613*, 66–70. https://doi.org/10.1038/s41586-022-05399-1.
23. Wang, Q.; Nakabayashi, M.; Hisatomi, T.; Sun, S.; Akiyama, S.; Wang, Z.; Pan, Z.; Xiao, X.; Watanabe, T.; Yamada, T.; Shibata, N.; Takata, T.; Domen, K. Oxysulfide Photocatalyst for Visible-Light-Driven Overall Water Splitting. *Nature Materials* **2019**, *18*, 827–832. https://doi.org/10.1038/s41563-019-0399-z.
24. Goto, Y.; Hisatomi, T.; Wang, Q.; Higashi, T.; Ishikiriyama, K.; Maeda, T.; Sakata, Y.; Okunaka, S.; Tokudome, H.; Katayama, M.; Akiyama, S.; Nishiyama, H.; Inoue, Y.; Takewaki, T.; Setoyama, T.; Minegishi, T.; Takata, T.; Yamada, T.; Domen, K. A Particulate Photocatalyst Water-Splitting Panel for Large-Scale Solar Hydrogen Generation. *Joule* **2018**, *2*, 509–520. https://doi.org/10.1016/j.joule.2017.12.009.
25. Maeda, K.; Xiong, A.; Yoshinaga, T.; Ikeda, T.; Sakamoto, N.; Hisatomi, T.; Takashima, M.; Lu, D.; Kanehara, M.; Setoyama, T.; Teranishi, T.; Domen, K. Photocatalytic Overall Water Splitting Promoted by Two Different Cocatalysts for Hydrogen and Oxygen Evolution under Visible Light. *Angewandte Chemie - International Edition* **2010**, *49*, 4096–4099. https://doi.org/10.1002/anie.201001259.
26. Zhang, G.; Lan, Z. A.; Lin, L.; Lin, S.; Wang, X. Overall Water Splitting by Pt/g-C3N4 Photocatalysts without Using Sacrificial Agents. *Chem Sci* **2016**, *7*, 3062–3066. https://doi.org/10.1039/c5sc04572j.
27. Liu, C.; Tang, J.; Chen, H. M.; Liu, B.; Yang, P. A Fully Integrated Nanosystem of Semiconductor Nanowires for Direct Solar Water Splitting. *Nano Lett* **2013**, *13*, 2989–2992. https://doi.org/10.1021/nl401615t.
28. Xu, J.; Pan, C.; Takata, T.; Domen, K. Photocatalytic Overall Water Splitting on the Perovskite-Type Transition Metal Oxynitride CaTaO2N under Visible Light Irradiation. *Chemical Communications* **2015**, *51*, 7191–7194. https://doi.org/10.1039/c5cc01728a.
29. Maeda, K.; Lu, D.; Domen, K. Direct Water Splitting into Hydrogen and Oxygen under Visible Light by Using Modified Taon Photocatalysts with D0 Electronic Configuration. *Chemistry - A European Journal* **2013**, *19*, 4986–4991. https://doi.org/10.1002/chem.201300158.

30. Bai, Y.; Li, C.; Liu, L.; Yamaguchi, Y.; Bahri, M.; Yang, H.; Gardner, A.; Zwijnenburg, M. A.; Browning, N. D.; Cowan, A. J.; Kudo, A.; Cooper, A. I.; Sprick, S. *Photocatalytic Overall Water Splitting Under Visible Light Enabled by a Particulate Conjugated Polymer Loaded with Palladium and Iridium*. 2022. https://doi.org/10.26434/chemrxiv-2022-8vr18.
31. Li, Z.; Li, R.; Jing, H.; Xiao, J.; Xie, H.; Hong, F.; Ta, N.; Zhang, X.; Zhu, J.; Li, C. Blocking the Reverse Reactions of Overall Water Splitting on a Rh/GaN–ZnO Photocatalyst Modified with Al2O3. *Nat Catal* **2023**, *6*, 80–88. https://doi.org/10.1038/s41929-022-00907-y.
32. Trasatti, S. Work Function, Electronegativity, and Electrochemical Behaviour of Metals. *J Electroanal Chem Interfacial Electrochem* **1972**, *39*, 163–184. https://doi.org/10.1016/S0022-0728(72)80485-6.
33. Yang, J.; Wang, D.; Han, H.; Li, C. Roles of Cocatalysts in Photocatalysis and Photoelectrocatalysis. *Acc Chem Res* **2013**, *46*, 1900–1909. https://doi.org/10.1021/ar300227e.
34. Takata, T.; Pan, C.; Nakabayashi, M.; Shibata, N.; Domen, K. Fabrication of a Core-Shell-Type Photocatalyst via Photodeposition of Group IV and v Transition Metal Oxyhydroxides: An Effective Surface Modification Method for Overall Water Splitting. *J Am Chem Soc* **2015**, *137*, 9627–9634. https://doi.org/10.1021/jacs.5b04107.
35. Wang, Q.; Hisatomi, T.; Jia, Q.; Tokudome, H.; Zhong, M.; Wang, C.; Pan, Z.; Takata, T.; Nakabayashi, M.; Shibata, N.; Li, Y.; Sharp, I. D.; Kudo, A.; Yamada, T.; Domen, K. Scalable Water Splitting on Particulate Photocatalyst Sheets with a Solar-to-Hydrogen Energy Conversion Efficiency Exceeding 1%. *Nat Mater* **2016**, *15*, 611–615. https://doi.org/10.1038/nmat4589.
36. Cui, Y.; Sheng, X.; Anusuyadevi, R.; Lawoko, M.; Svagan, A. J. Self-Assembled Carbon Spheres Prepared from Abundant Lignin and Urea for Photocatalytic and Self-Propelling Applications. *Carbon Trends* **2021**, *3*, 40. https://doi.org/10.1016/j.cartre.2021.10.
37. Wang, D.; Li, R.; Zhu, J.; Shi, J.; Han, J.; Zong, X.; Li, C. Photocatalytic Water Oxidation on BiVO 4 with the Electrocatalyst as an Oxidation Cocatalyst: Essential Relations between Electrocatalyst and Photocatalyst. *Journal of Physical Chemistry C* **2012**, *116*, 5082–5089. https://doi.org/10.1021/jp210584b.
38. Maeda, K.; Wang, X.; Nishihara, Y.; Lu, D.; Antonietti, M.; Domen, K. Photocatalytic Activities of Graphitic Carbon Nitride Powder for Water Reduction and Oxidation under Visible Light. *Journal of Physical Chemistry C* **2009**, *113*, 4940–4947. https://doi.org/10.1021/jp809119m.
39. Kasahara, A.; Nukumizu, K.; Hitoki, G.; Takata, T.; Kondo, J. N.; Hara, M.; Kobayashi, H.; Domen, K. Photoreactions on LaTiO 2 N under Visible Light Irradiation. *J. Phys. Chem. A* **2002**, *106*, 6750–6753. https://doi.org/10.1021/jp025961.
40. Ma, B.; Yang, J.; Han, H.; Wang, J.; Zhang, X.; Li, C. Enhancement of Photocatalytic Water Oxidation Activity on Iro X-Zno/Zn2-Xgeo4-x-3yn2y Catalyst with the Solid Solution Phase Junction. *Journal of Physical Chemistry C* **2010**, *114*, 12818–12822. https://doi.org/10.1021/jp103722j.
41. Rosman, N. N.; Yunus, R. M.; Shah, N. R. A. M.; Shah, R. M.; Arifin, K.; Minggu, L. J.; Ludin, N. A. An Overview of Co-Catalysts on Metal Oxides for Photocatalytic Water Splitting. *International Journal of Energy Research* **2022**, *46*, 11596–11619. https://doi.org/10.1002/er.8001.

42. Maeda, K.; Domen, K. Photocatalytic Water Splitting: Recent Progress and Future Challenges. *Journal of Physical Chemistry Letters* **2010**, *1*, 2655–2661. https://doi.org/10.1021/jz1007966.
43. Lakhera, S. K.; Rajan, A.; T.P., R.; Bernaurdshaw, N. A Review on Particulate Photocatalytic Hydrogen Production System: Progress Made in Achieving High Energy Conversion Efficiency and Key Challenges Ahead. *Renewable and Sustainable Energy Reviews* **2021**, *152*, 111694. https://doi.org/10.1016/j.rser.2021.111694.
44. Xing, Z.; Zong, X.; Pan, J.; Wang, L. On the Engineering Part of Solar Hydrogen Production from Water Splitting: Photoreactor Design. *Chemical Engineering Science* **2013**, *104*, 125–146. https://doi.org/10.1016/j.ces.2013.08.039.
45. Wang, X.; Liu, G.; Chen, Z. G.; Li, F.; (Max) Lu, G. Q.; Cheng, H. M. Efficient and Stable Photocatalytic H2 Evolution from Water Splitting by (Cd0.8Zn0.2)S Nanorods. *Electrochem commun* **2009**, *11*, 1174–1178. https://doi.org/10.1016/j.elecom.2009.03.041.
46. Anusuyadevi, P. R.; Riazanova, A. V.; Hedenqvist, M. S.; Svagan, A. J. Floating Photocatalysts for Effluent Refinement Based on Stable Pickering Cellulose Foams and Graphitic Carbon Nitride (g-C3n4). *ACS Omega* **2020**, *5*, 22411–22419. https://doi.org/10.1021/acsomega.0c02872.
47. Jing, D.; Liu, H.; Zhang, X.; Zhao, L.; Guo, L. Photocatalytic Hydrogen Production under Direct Solar Light in a CPC Based Solar Reactor: Reactor Design and Preliminary Results. *Energy Convers Manag* **2009**, *50*, 2919–2926. https://doi.org/10.1016/j.enconman.2009.07.012.
48. Yasuda, M.; Matsumoto, T.; Yamashita, T. Sacrificial Hydrogen Production over TiO2-Based Photocatalysts: Polyols, Carboxylic Acids, and Saccharides. *Renewable and Sustainable Energy Reviews* **2018**, *81*, 1627–1635. https://doi.org/10.1016/j.rser.2017.05.243.
49. Chen, S.; Takata, T.; Domen, K. Particulate Photocatalysts for Overall Water Splitting. *Nat Rev Mater* **2017**, *2*. https://doi.org/10.1038/natrevmats.2017.50.
50. Fontelles-Carceller, O.; Muñoz-Batista, M. J.; Conesa, J. C.; Kubacka, A.; Fernández-García, M. H2 Photo-Production from Methanol, Ethanol and 2-Propanol: Pt-(Nb)TiO2 Performance under UV and Visible Light. *Molecular Catalysis* **2018**, *446*, 88–97. https://doi.org/10.1016/j.mcat.2017.12.023.
51. Maeda, K.; Higashi, M.; Lu, D.; Abe, R.; Domen, K. Efficient Nonsacrificial Water Splitting through Two-Step Photoexcitation by Visible Light Using a Modified Oxynitride as a Hydrogen Evolution Photocatalyst. *J Am Chem Soc* **2010**, *132*, 5858–5868. https://doi.org/10.1021/ja1009025.
52. Nalajala, N.; Patra, K. K.; Bharad, P. A.; Gopinath, C. S. Why the Thin Film Form of a Photocatalyst Is Better than the Particulate Form for Direct Solar-to-Hydrogen Conversion: A Poor Man's Approach. *RSC Adv* **2019**, *9*, 6094–6100. https://doi.org/10.1039/c8ra09982k.
53. Anusuyadevi, P. R.; Svagan, A. J. Role of Cellular Solids in Heterogeneous Photocatalytic Applications. In *Nanostructured Photocatalysts: From Fundamental to Practical Applications*; Elsevier, 2021; pp 305–330. https://doi.org/10.1016/B978-0-12-823007-7.00017-1.
54. Tudu, B.; Nalajala, N.; Reddy, K.; Saikia, P.; Gopinath, C. S. Electronic Integration and Thin Film Aspects of Au-Pd/RGO/TiO2 for Improved Solar Hydrogen Generation. *ACS Appl Mater Interfaces* **2019**, *11*, 32869–32878. https://doi.org/10.1021/acsami.9b07070.

55. Tudu, B.; Nalajala, N.; Saikia, P.; Gopinath, C. S. Cu–Ni Bimetal Integrated TiO2 Thin Film for Enhanced Solar Hydrogen Generation. *Solar RRL* **2020**, *4*. https://doi.org/10.1002/solr.201900557.
56. Mani, S. S.; Rajendran, S.; Nalajala, N.; Mathew, T.; Gopinath, C. S. Electronically Integrated Mesoporous Ag–TiO2 Nanocomposite Thin Films for Efficient Solar Hydrogen Production in Direct Sunlight. *Energy Technology* **2022**, *10*. https://doi.org/10.1002/ente.202100356.
57. Schröder, M.; Kailasam, K.; Borgmeyer, J.; Neumann, M.; Thomas, A.; Schomäcker, R.; Schwarze, M. Hydrogen Evolution Reaction in a Large-Scale Reactor Using a Carbon Nitride Photocatalyst under Natural Sunlight Irradiation. *Energy Technology* **2015**, *3*, 1014–1017. https://doi.org/10.1002/ente.201500142.
58. Hisatomi, T.; Domen, K. Reaction Systems for Solar Hydrogen Production via Water Splitting with Particulate Semiconductor Photocatalysts. *Nature Catalysis* **2019**, *2*, 387–399. https://doi.org/10.1038/s41929-019-0242-6.
59. Nishiyama, H.; Yamada, T.; Nakabayashi, M.; Maehara, Y.; Yamaguchi, M.; Kuromiya, Y.; Nagatsuma, Y.; Tokudome, H.; Akiyama, S.; Watanabe, T.; Narushima, R.; Okunaka, S.; Shibata, N.; Takata, T.; Hisatomi, T.; Domen, K. Photocatalytic Solar Hydrogen Production from Water on a 100-M2 Scale. *Nature* **2021**, *598*, 304–307. https://doi.org/10.1038/s41586-021-03907-3.
60. Cox, N.; Pantazis, D. A.; Neese, F.; Lubitz, W. Artificial Photosynthesis: Understanding Water Splitting in Nature. *Interface Focus* **2015**, *5*, 1–10. https://doi.org/10.1098/rsfs.2015.0009.
61. Kärkäs, M. D.; Verho, O.; Johnston, E. V.; Åkermark, B. Artificial Photosynthesis: Molecular Systems for Catalytic Water Oxidation. *Chemical Reviews* **2014**, *114*, 11863–12001. https://doi.org/10.1021/cr400572f.
62. James, B. D.; Baum, G. N.; Perez, J.; Baum, K. N. *Technoeconomic Analysis of Photoelectrochemical (PEC) Hydrogen Production Final Report Technoeconomic Analysis for Photoelectrochemical Hydrogen Production 2*; 2009. https://www.osti.gov/biblio/1218403 (accessed 2024-02-22).
63. Pinaud, B. A.; Benck, J. D.; Seitz, L. C.; Forman, A. J.; Chen, Z.; Deutsch, T. G.; James, B. D.; Baum, K. N.; Baum, G. N.; Ardo, S.; Wang, H.; Miller, E.; Jaramillo, T. F. Technical and Economic Feasibility of Centralized Facilities for Solar Hydrogen Production via Photocatalysis and Photoelectrochemistry. *Energy Environ Sci* **2013**, *6*, 1983–2002. https://doi.org/10.1039/c3ee40831k.
64. Bala Chandran, R.; Breen, S.; Shao, Y.; Ardo, S.; Weber, A. Z. Evaluating Particle-Suspension Reactor Designs for Z-Scheme Solar Water Splitting via Transport and Kinetic Modeling. *Energy Environ Sci* **2018**, *11*, 115–135. https://doi.org/10.1039/c7ee01360d.
65. Wang, Z.; Li, C.; Domen, K. Recent Developments in Heterogeneous Photocatalysts for Solar-Driven Overall Water Splitting. *Chemical Society Reviews* **2019**, *48*, 2109–2125. https://doi.org/10.1039/c8cs00542g.
66. Sayama, K.; Miseki, Y. Research and Development of Solar Hydrogen Production- Toward the Realization of Ingenious Photocatalysis-Electrolysis Hybrid System. *Translations from Synthesiology* **2014**, *7*, 81–92.
67. Zhao, Y.; Ding, C.; Zhu, J.; Qin, W.; Tao, X.; Fan, F.; Li, R.; Li, C. A Hydrogen Farm Strategy for Scalable Solar Hydrogen Production with Particulate Photocatalysts. *Angewandte Chemie - International Edition* **2020**, *59*, 9653–9658. https://doi.org/10.1002/anie.202001438.

68. Rashid, M.; Khaloofah, M.; Mesfer, A.; Naseem, H.; Danish, M.; Al Mesfer, M. K. *Hydrogen Production by Water Electrolysis: A Review of Alkaline Water Electrolysis, PEM Water Electrolysis and High Temperature Water Electrolysis* 2015. https://www.researchgate.net/publication/273125977 (accessed 2024-02-28),
69. Wang, Q.; Domen, K. Particulate Photocatalysts for Light-Driven Water Splitting: Mechanisms, Challenges, and Design Strategies. *Chemical Reviews.* **2020**, *120*, 919–985. https://doi.org/10.1021/acs.chemrev.9b00201.
70. Li, R.; Li, C. Scalable Solar Water Splitting Using Particulate Photocatalysts. *Current Opinion in Green and Sustainable Chemistry* **2022**, *33*, 100577. https://doi.org/10.1016/j.cogsc.2021.100577.
71. Ahsan, S. S.; Gumus, A.; Erickson, D. Redox Mediated Photocatalytic Water-Splitting in Optofluidic Microreactors. *Lab Chip* **2013**, *13*, 409–414. https://doi.org/10.1039/c2lc41129f.
72. Li, L.; Chen, R.; Liao, Q.; Zhu, X.; Wang, G.; Wang, D. High Surface Area Optofluidic Microreactor for Redox Mediated Photocatalytic Water Splitting. *International Journal of Hydrogen Energy* **2014**, *39*, 19270–19276. https://doi.org/10.1016/j.ijhydene.2014.05.098.
73. Pala, L. P. R.; Peela, N. R. Visible Light Active IrO2/TiO2 Films for Oxygen Evolution from Photocatalytic Water Splitting in an Optofluidic Planar Microreactor. *Renew Energy* **2022**, *197*, 902–910. https://doi.org/10.1016/j.renene.2022.08.017.
74. Gong, L.; Chu, Q.; Liu, X.; Tan, Y. Plasmonic Platinum Nanoparticles-Tungsten Oxide Nanoarchitectures as Visible Light Photocatalysts for Highly Efficient Overall Water Splitting. *J Mater Chem A Mater* **2022**, *10*, 21161–21176. https://doi.org/10.1039/d2ta05184b.
75. Weng, B.; Qi, M. Y.; Han, C.; Tang, Z. R.; Xu, Y. J. Photocorrosion Inhibition of Semiconductor-Based Photocatalysts: Basic Principle, Current Development, and Future Perspective. *ACS Catalysis* **2019**, *9*, 4642–4687. https://doi.org/10.1021/acscatal.9b00313.
76. Wang, C.; Wang, L.; Jin, J.; Liu, J.; Li, Y.; Wu, M.; Chen, L.; Wang, B.; Yang, X.; Su, B. L. Probing Effective Photocorrosion Inhibition and Highly Improved Photocatalytic Hydrogen Production on Monodisperse PANI@CdS Core-Shell Nanospheres. *Appl Catal B* **2016**, *188*, 351–359. https://doi.org/10.1016/j.apcatb.2016.02.017.
77. Han, C.; Yang, M. Q.; Weng, B.; Xu, Y. J. Improving the Photocatalytic Activity and Anti-Photocorrosion of Semiconductor ZnO by Coupling with Versatile Carbon. *Physical Chemistry Chemical Physics* **2014**, *16*, 16891–16903. https://doi.org/10.1039/c4cp02189d.
78. Christoforidis, K. C.; Fornasiero, P. Photocatalysis for Hydrogen Production and CO2 Reduction: The Case of Copper-Catalysts. *ChemCatChem* **2019**, *11*, 368–382. https://doi.org/10.1002/cctc.201801198.
79. Ning, X.; Lu, G. Photocorrosion Inhibition of CdS-Based Catalysts for Photocatalytic Overall Water Splitting. *Nanoscale* **2020**, *12*, 1213–1223. https://doi.org/10.1039/c9nr09183a.
80. Tian, B.; Gao, W.; Zhang, X.; Wu, Y.; Lu, G. Water Splitting over Core-Shell Structural Nanorod CdS@Cr2O3 Catalyst by Inhibition of H2-O2 Recombination via Removing Nascent Formed Oxygen Using Perfluorodecalin. *Appl Catal B* **2018**, *221*, 618–625. https://doi.org/10.1016/j.apcatb.2017.09.065.